MARINE PLASTIC DRIFT FROM THE MEKONG RIVER TO SOUTHEAST ASIA

Author: Nguyen Manh Dung

Supervisor: Dr. Lars Robert Hole
Co-supervisors: Dr. Øyvind Breivik
Dr. Mari Skuggedal Myksvoll

Master's Thesis in Physical Oceanography
Geophysical Institute, University of Bergen

November 20, 2022

Acknowledgements

I would like to express my sincere thanks to NORAD (Norwegian agency for development cooperation) for long term support of the collaboration between Vietnam and Norway on marine forecasting. This long-term support has helped the Vietnam Meteorological and Hydrological Administration to have great breakthroughs in marine research and forecasting, including waves, currents, tides, storm surges, and free and good quality forecasting and observation resources.

I would like to thank my supervisor, Dr. Lars Robert Hole (Meteorological Institute), for the great guidance and friendship we have been sharing over these two last years. Thank you for trusting on my capacity and providing so many resources that helped me to come and continue studying in Bergen.

My special thanks to my co-supervisors Dr. Øyvind Breivik (Meteorological Institute) and Dr. Mari Skuggedal Myksvoll (Institute of Marine Research) for guiding me over the development of this thesis and your helpful comments.

I also dedicate this work to my co-workers from the Norwegian Meteorological Institute, in special Knut-Frode for the technical supports on OpenDrift and the scientific discussions, and Georgios Magklaras for technical support on PPI.

I also would like to thank Prithvinath Madduri (PhD student at Geophysical Institute) for technical supports on OpenDrift and the scientific discussions for my thesis.

In addition, my sincere thanks to my former colleagues from the Vietnam Meteorological and Hydro-logical Administration, especially Nguyen Manh Linh for technical supports on Linux system, and Nguyen Ngoc Hoa and Le Thi Oanh for useful information on the Mekong river.

Last but not least, to my beloved family, former colleagues and friends in Vietnam, those supported and embraced me despite the long distance.

Nguyen Manh Dung
Bergen, November 20, 2022

Abstract

Plastic waste has been identified as a major worldwide environmental issue (*Sun et al.*, 2021; *Zhang et al.*, 2020). It affects the marine environment and human activities (*Sun et al.*, 2021). *Jambeck et al.* (2015) estimated that between 4.8 and 12.7 million tons of plastic waste entering the ocean every year. A major share of this amount originates in the countries of Southeast Asia (*Harris et al.*, 2021; *Sun et al.*, 2021). The South China Sea, the biggest sea in Southeast Asia, is surrounded by six out of the ten biggest marine plastics contributors. Mekong is the greatest river in the South China Sea, and it is ranked between 8th and 11st biggest plastics contributor to the oceans (*Haberstroh et al.*, 2021). Therefore, it is important to examine how plastic drift from Mekong river to the South China Sea and its surrounding waters in both short terms (3 months) and long term (15 months). I also examine the potential factors (stranding, river, river frequency, wind drift, vertical mixing and biofouling) that can affect the trajectory of plastic particles. There are several findings. Firstly, the seasonal drift is influenced by the monsoon systems that during the summer the plastic particles drift mainly to the northeast, and in the winter they drift to the southwest. Secondly, in the long term, the particles drift to all seas and straits across Southeast Asia, some of them leak to the Pacific and Indian oceans, and the Philippines is most vulnerable to plastic pollution. Thirdly, if considering stranding, most of the plastics (97%) are stranded after 15 months, the average travelling time is 3.7 months, and again the Philippines is most vulnerable to marine plastic pollution. Next, rivers play a role in dispersing plastic waste; however, their influences are mainly in the area around the rivers and for a short time. Wind drift and vertical mixing can have combined effects on the trajectory of marine plastics. Wind drift plays an important role in pushing water particles right at the surface, while vertical mixing is particularly important in the vertical distribution of the particles. Lastly, biofouling simulations with terminal velocities of 1, 2, 5 meters/day show that plastic particles mostly deposit in the southern continental shelf of the South China Sea where the water is shallow (below 150m). Many particles are suspended in the deep waters in the middle of the South China Sea.

List of abbreviations

1. **CMEMS** The Copernicus Marine Environment Monitoring Service (the Copernicus Marine Service)
2. **ECMWF** The European Centre for Medium-Range Weather Forecasts
3. **EFAS** The European Flood Awareness System
4. **HPC** High-performance computing
5. **MET** The Norwegian Meteorological Institute
6. **NCHMF** The Vietnam National Center for Hydro-Meteorological Forecasting
7. **PPI** Post-Processing Infrastructure
8. **ROMS** The Regional Ocean Modeling System, The Vietnam ROMS3D
9. **SCS** South China Sea, the South China Sea
10. **SEA** Southeast Asia
11. **VNMHA** The Vietnam Meteorological and Hydro-logical Administration

Contents

List of Figures

Chapter 1

INTRODUCTION

1.1 Problem

Plastic waste has been identified as a major worldwide environmental issue (*Sun et al.*, 2021; *Zhang et al.*, 2020). It affects the marine environment and human activities (*Md Amin et al.*, 2020; *Sun et al.*, 2017). For example, plastics were found in the stomach of green turtles in Hongkong (*Ng et al.*, 2016) and in sea birds in the South China Sea (*Zhu et al.*, 2019). Plastic waste also damages marine landscapes and tourism (*Sun et al.*, 2021; *Zhang et al.*, 2020). Jambeck and others estimated that between 4.8 and 12.7 million tons of plastic waste entering the ocean every year (*Jambeck et al.*, 2015), contributing to six giant garbage patches, and those patches increase in size over time. A major share of plastic waste entering the ocean patches originates in the countries of Southeast Asia, mostly through their rivers (*Harris et al.*, 2021; *Sun et al.*, 2021). According to an estimate, Asian rivers may contribute up to 86% of the marine plastics (*Haberstroh et al.*, 2021). In addition, countries bordering the South China Sea (SCS) may contribute 2.56–7.08 million tons of plastic waste to the oceans yearly (*Jambeck et al.*, 2015). It is worth mentioning that six (China, Indonesia, Philippines, Vietnam, Thailand and Malaysia) of the countries bordering the SCS are among the ten biggest marine plastics contributors (fig. A1). Mekong, the greatest river in the SCS, is ranked between the 8th and the 11st biggest plastic contributor to the oceans (*Haberstroh et al.*, 2021). This is because three (China, Vietnam and Thailand) of six Mekong countries are among of the ten biggest marine plastics contributors.

1.2 Motivation

Although the Mekong river is the biggest river in the SCS, and the SCS is surrounded by six out of ten biggest marine plastic contributors, there have been no studies on how marine waste drifts from the Mekong river to Southeast Asia. Therefore, it is important to examine this drifting and the potential factors affecting the drifting.

There are many factors that control the drifting in the SCS and SEA. Firstly, the SCS is semi-enclosed, and mainly influenced by the monsoon system, in which the northeasterly monsoon prevails in the winter and the southwesterly monsoon prevails in the summer.

Secondly, the stranding of plastic particles can affect the drifting of plastics. This

stranding depends on both the particles and the coast. For example, the shape, size and buoyancy of the particles, and the features of the coast including vegetation, sediments, rocks greatly influence the stranding and the return back to the sea. Beach characteristics like steepness and sediment type could determine which particles are stranded (*Van Sebille et al.*, 2020).

Thirdly, rivers may play a role in distributing plastics because rivers carry freshwater to the sea. They generate eddies (*Cushman-Roisin*, 2011) that carry plastic particles. Rivers also carry plastics to the sea (*Haberstroh et al.*, 2021; *Harris et al.*, 2021; *Sun et al.*, 2021). In the Mekong River plastic waste mostly floats on the surface and drifts to the sea during the flood season *Haberstroh et al.* (2021).

Next, the accuracy of simulations depends not only on the background currents (i.e., geostrophic, tidal, baroclinic currents), but also depends significantly on the wind-driven drift current (*van der Mheen et al.*, 2020). The wind drift current have two components, which are Stokes drift and wind-induced shear current. Stokes drift decays exponentially with depth, and at the surface Stockes drift makes up to around 1 or 2% of the wind speed (*van der Mheen et al.*, 2020). Whereas, the understanding of the wind-induced shear current is controversial. Usually, the wind drift current is parameterized, called wind (drift) factor. The wind drift factor make up between 1 and 6 % of the wind. However, depending on each different object, this parameter is adjusted.

The vertical mixing also can play a role in the distribution of buoyant particles (*Kooi et al.*, 2016; *Kukulka et al.*, 2012; *Röhrs et al.*, 2018). This brings plastic particles up and down in the water column, and the vertical positions of the particles can affect the horizontal drift. The vertical mixing is caused by several factors including cooling, waves, winds, tides and buoyancy. In practice, it is parameterized, for example a constant vertical diffusivity.

The last factor is the deposition of marine plastics. Specifically, plastics is often accumulated in landfills, and then follow the runoff to rivers and the seas. Plastics can be broken into smaller pieces (micro-plastics) due to weathering and physical forces (*Van Sebille et al.*, 2020). Micro-plastics would sink if its density is greater than that of sea water such as polystyrene (PS). However, in the seabed sediments, there are also plastic particles which is lighter than seawater, such as polyethylene (PE) (*Kaiser et al.*, 2017). *Barrett et al.* (2020) states that the amount of marine plastic deposited on the seafloor increases in proportion to the increase in the amount of floating marine plastic on the sea surface. It is estimated that there are 14 million tonnes of microplatics in the ocean floors (*Barrett et al.*, 2020). The estimate is highly variable, and significantly higher than recorded in other analysis (*Barrett et al.*, 2020).

There are several processes that sink light marine plastics. For example, microplastics can sink when it is stick to marine snow (organic detritus). They also can be eaten by marine animals (*Van Sebille et al.*, 2020; *Zhu et al.*, 2019) and sink with their fecal pellets. Giant larvaceans and zooplankton also can carry plastic particles to the bottom. Suspended inorganic particles such as clay can increase the weight of plastics and sink. Extreme events including earthquakes, cyclones and floods can also transport plastic particles to the bottom. Biofouling is also one of the processes that deposit microplastics (*Kaiser et al.*, 2017; *Lobelle et al.*, 2021; *Van Sebille et al.*, 2020).

Biofouling is the growing of organisms on plastic particles which adds mass, causes changes in overall buoyancy of the bio-fouled particle, increasing settling velocity (*Kaiser et al.*, 2017; *Lobelle et al.*, 2021). In the equatorial Pacific the sinking of

microplastics is more dependent on biofouling (*Lobelle et al.*, 2021). If the density of plastic particles is greater than seawater, it sinks down to the deeper layers until it reaches the bottom or suspended in the layer of corresponding buoyancy. This deposition (biofouling) depends on many factors such as density, shape, salinity, particle size (*Lobelle et al.*, 2021). Biofouling also depends on the duration in sea water. According to *Kaiser et al.* (2017) PE does not sink after 14 weeks in estuary but start to sink after 6 weeks in coastal water.

Our understanding of the sinking rate is relatively limited. Different approaches give very different numbers. One of the approaches is to calculate according to the mathematical formula Stokes Law. In this calculation, it is assumed that the object is spherical, the density of the object are constant, and the terminal velocity depends on the density of the water, gravity, the density of the object, the viscosity and the size (radius) of the object. This result shows that the larger the object, the greater the terminal velocity. However, this approach is purely mathematical and the object is usually not spherical. In addition, sinking velocities of irregularly shaped particles were considerably lower than theoretical values for spheres (*Kaiser et al.*, 2019).

Kaiser et al. (2019) calculated the terminal velocities of spherical PS particles with sizes from 0.02mm to 0.1mm under various conditions. The results indicate that the terminal velocities range from 0.62 to 18.87 m/d. In addition, experiments conducted with different plastic particles in different salinity environments show that particle sizes ranged from 0.3 and 3.6mm sink with velocities between 6 and 91 mm/s (or 518 and 7864 m/d, respectively) (*Kowalski et al.*, 2016).

In biofouling, the density of the objects increase over time that the core (plastics) is lighter than seawater and unchanged, and the cover (algae) is heavier than seawater and increase in time. Two objects different in size initially have the same density and lighter than seawater. Over time during the biological process, the two objects are covered by algae which is heavier than seawater. Consequently, the larger object will gain more weight due to more surface area. In contrast, the small object gain less mass due to less surface area, but its density increases more than the larger object. As a result, the smaller particle sink first. One evidence is that *Kooi et al.* (2017) indicated that there is a lack of small particles observed at the ocean surface, or particles smaller than 1 mm are somehow “lost”. *Lobelle et al.* (2021) explains that "the smaller the object is, the greater the relative surface area is". "Due to a trade-off between the collision frequency with algae and surface-to-volume ratio, the smallest particles (0.1 micrometer) start sinking immediately and the larger particles (0.1–10 mm) taken around 30 days to start sinking" *Lobelle et al.* (2021). Although the smallest particles sink first, many of them may never reach the sea floor and remain suspended in the intermediate water (*Kooi et al.*, 2017).

1.3 Objectives

The purpose of this research is to examine how plastic drift from Mekong river to the South China Sea and its surrounding seas, straits and oceans. I also examine the potential factors that can affect the trajectory of plastic particles. Specifically, I look at the drifting in both short terms (3 months) for the summer and the winter and long term (15 months). Additionally, I investigate the effects of stranding, river, river frequency,

wind drift, vertical mixing and biofouling on plastic drifting.

In this research, I use a number of data sources and tools for simulations. Firstly, the OpenDrift model developed by MET is used for the simulations. This model requires wind, and ocean current as the inputs. Wind data is downloaded from CMEMS, while I run Vietnam ROMS3D to simulate 3D ocean currents. However, ROMS domain covers only the South China Sea (fig. A2); therefore, for the areas outside the ROMS domain, I use the ocean currents downloaded from CMEMS (fig. A3).

The document is structured as follows: Chapter 2 presents the study area, and the main forces acting on this area (winds, waves, currents) and around the Mekong mouths (tides and river water). Chapter 3 covers three parts, part one is the data sources used in this research, part two presents the models and clarify the methodology, and the last part is model validation including OpenDrift, ROMS and river discharge rates. Chapter 4 shows detailed methods with assumptions, and then the results of simulations. Chapter 5 discuss the results and assumptions. Chapter 6 synthesizes the study and presents limitations of the simulations in this research.

Chapter 2

STUDY AREA

2.1 Southeast Asia

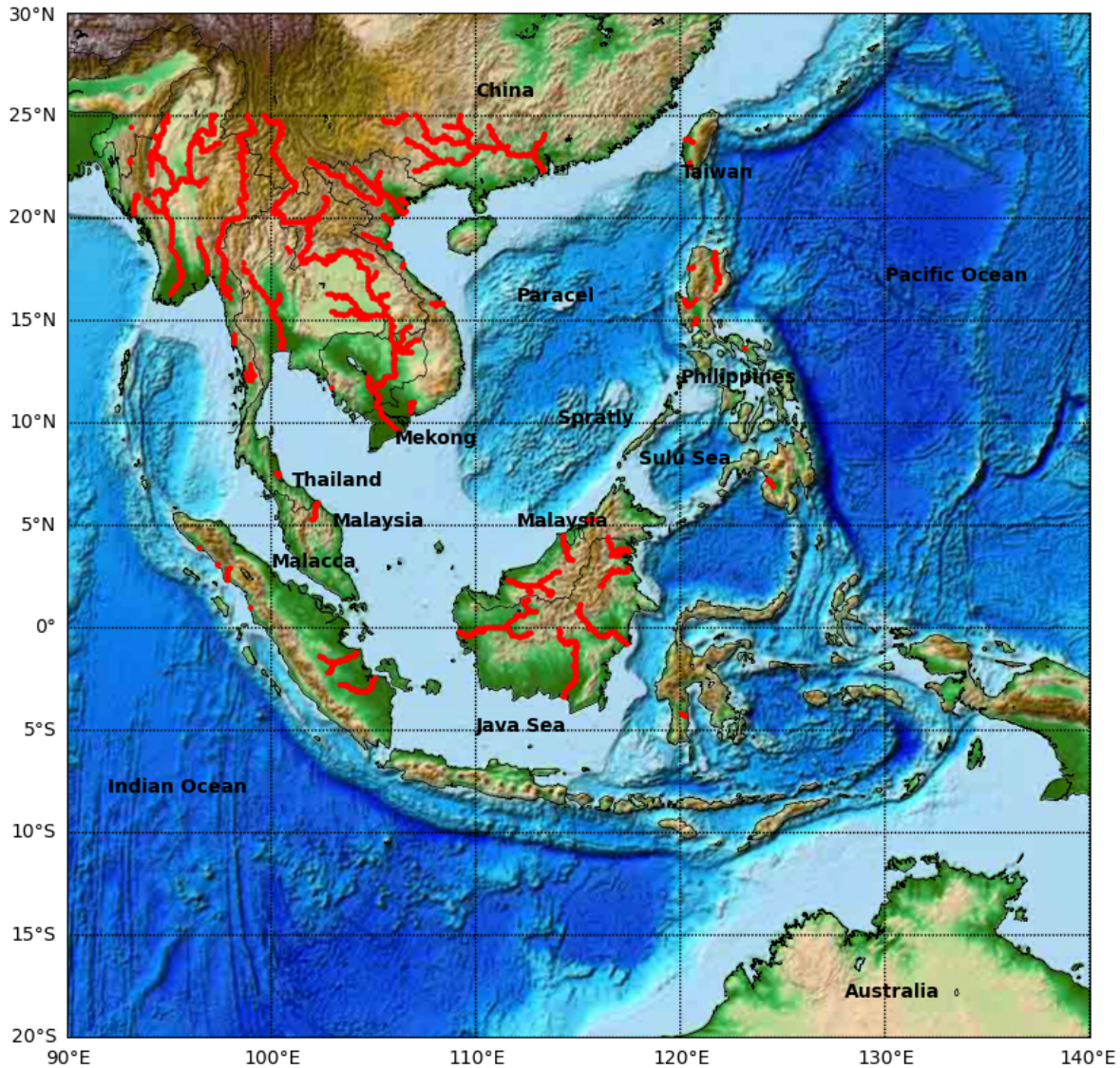

Figure 2.1: Study area with major rivers shown as red lines.

The study area is Southeast Asia, or the South China Sea and its surrounding waters from latitude 20°S to 30°N, and longitude from 90°E to 140°E. There are several rivers in the study area. The red lines in fugure 2.1 represent the largest rivers in Southeast Asia. Among the rivers around the South China Sea, the three largest rivers are the Mekong river (South of Vietnam), the Truong Giang river (South of China) and the Red river (North of Vietnam) with the maximum of over 40.000, 20.000, and 8.000 m^3/s, respectively. These rivers account for most of the total river discharge to the South China Sea, see figure A4. In term of bathymetry, the north, west and south of the SCS are shallow, mostly below 150 meters while the middle and the east of the SCS are relatively deep, between 1000 and 5000 meter depth.

2.2 Wind and its influence

The South China Sea is influenced by the monsoon system. In the summer, the southwesterly monsoon (225 degree) with average speed of 4-5m/s creates waves between 0.5 and 1.0m. In winter, the strong northeasterly monsoon (45 degree) with average speed of 8-10m/s generates waves about 1.5-2.0m. These data can be seen in figures A5 and A6. Around the Mekong mouths, in the winter the northeasterly monsoon blows parallel to the shore, pushing the water toward the coast. This combines with the shape of the coast and shallow waters (10-30m) resulting in the increase of sea surface height (*Thuy et al.*, 2019). In contrast, in the summer, southwesterly winds blow parallel to the shore, driving the water seaward. This leads to the decrease in sea surface height and an up-welling for the area (*Kuo et al.*, 2000). Thus, sea surface height in the winter is greater than in the summer around Mekong mouths. The difference between the summer and the winter in sea water elevation is around 0.7m. This is also illustrated in figure A7 with the sea surface height in Vung Tau.

2.3 The main currents in the study area

The circulation at upper layers of the South China Sea are mainly influenced by the monsoon system. The northeasterly winds in the winter results in a cyclonic circulation while the prevailing winds in the summer create an anti-cyclonic circulation at the surface layer (fig. A8) (*Qi-zhou et al.*, 1994). The details of the currents in the SCS can be seen in figure A9. Although this figure is snapshots, in my experience, they are not changed much in a few months.

The South China Sea is semi-enclosed, and slightly affected by Kuroshio current in the East of the Philippines and Taiwan (*Qi-zhou et al.*, 1994). In the equator, the Indonesian seas, trade winds drive the surface water from east to west. It was hypothesized that this drives the Indonesian Throughflow (fig. A10) in the Indonesian Seas. However, a recent model suggested the Indonesian Throughflow is actually an extension of the Pacific's tropical current systems (*Mayer et al.*, 2010; *Taufiqurrahman et al.*, 2020).

2.4 The tides around Mekong deltas

The tidal range around Mekong river is large, and the tidal type is semi diurnal (*Thuy et al.*, 2019; *Trinh et al.*, 2020). However, I analyzed historical data from Vung Tau station for 13 months from 12/2020 to 12/2021 (see figure A11). The results show that the tidal type is mixed, mainly semi diurnal, and the tidal range is over 4m with the maximum around 430cm from late Autumn to the winter and the minimum is around 0 in the summer. This large tidal range might be important for mixing river water and sea water. Data at the Tan Chau and Chau Doc stations (see locations A12), near the border between Vietnam and Cambodia, 400 kilometers from shore, indicates that the flow is affected by the tides with much larger flows downstream than upstream. In the area of My Thuan and Can Tho (see locations A12), about 90 kilometers from shore, this influence is much more pronounced with a similarity between inflows and outflows in the dry season, and much larger outflows than inflows in the flood season.

2.5 River discharge rate

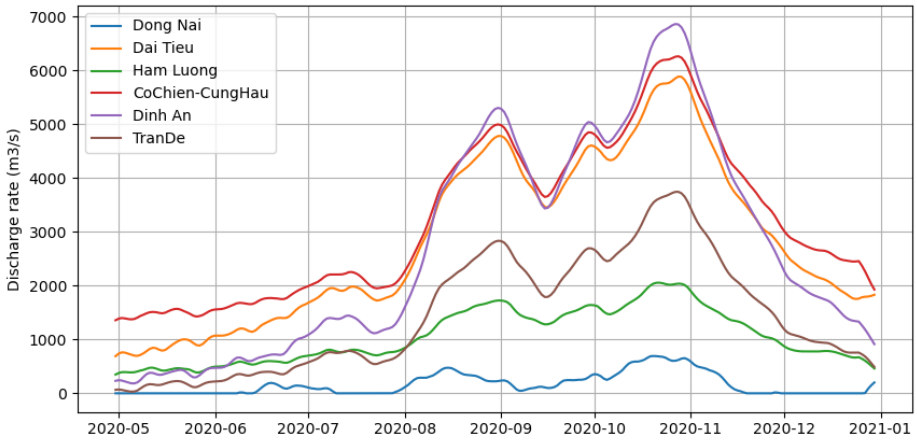

Figure 2.2: Runoff at Mekong mouths (red dots in fig. A12) during 2020

Flood stages in the Mekong River affect the transport of garbage to the sea. In the dry season, garbage accumulates in landfills. In the flood season, the garbage follows the runoff to the rivers, then to the sea, most clearly in the summer (*Haberstroh et al.*, 2021). According to VNHMA, the water discharge rate starts to increase from May, peaks in October, and then decreases to its minimum in April. Flood season as defined by VNHMA is from July to December and dry season from January to June. This also can be seen in figure 2.2. Although this is only one year of data for 2020 and other years might be different, the general trend is not much different. For example, figure A13 shows that in 2020 water started to increase sharply in August and peaks in October, while in 2021 it increased sharply in June and peaks also in October.

It should be noted that the Mekong River has six to nine mouths, and I divided them into six mouths (see red dots in figure A12) based on its geographical locations.

Chapter 3

METHODOLOGY

3.1 Methods

3.1.1 Lagrangian Particle Tracking

In fluid dynamics, the fluid motion can be described in two ways: the Eulerian or Lagrangrian approach. The Eulerian approach describes the motion of fluid at fixed points in space. This is the foundation method for most circulation models. This method is very practical in studying fluid motion in a location, such as the weather in a city, the water level at a port. In the Lagrangian method, a fluid mass is a collection of a great number of discrete water particles, and fluid motion is an accumulation of continuous water particles. Since simulating a great number of water particles consumes a lot of computer resource, this method is less practical in simulating the fluid motion. However, when studying the trajectories of a limited number of drifting objects (i.e., marine plastics, sea grass seeds, fish eggs, oil spill), the Lagrangian method is more practical. Lagrange approach is commonly used to simulate trajectories of drifting objects (*van der Mheen et al.*, 2020; *van Sebille et al.*, 2018). There are two techniques of Lagrangian integration: the online and the offline approach. In the online approach, the trajectories of objects are computed when data (i.e., velocity) in the Eulerian model is updated. Due to the instantaneous requirements, the online approach is not practical. In the offline trajectory calculations, trajectories are computed using stored velocity fields from the Eulerian model. This provides the ability to compute trajectories in both forward or backward modes in time (*van Sebille et al.*, 2018). For emergency purposes, offline models are often the only option that is fast enough to meet requirements such as search and recue purposes. Also, offline models can be peformed quickly without the need of rerunning the full Eulerian model (*Dagestad et al.*, 2018).

3.1.2 OpenDrift Model

OpenDrift is developed based on the offline Lagrangrian particle tracking method. It is an open source framework for ocean trajectory modeling and developed by the Norwegian Meteorological Institute (MET). This model is programmed in python and can be downloaded from https://opendrift.github.io/. It is designed to accommodate various types of drift calculations in the ocean or atmosphere. There are many modules have already been developed, for example, oil drift module, a search and rescue module, fish

eggs module, plastics drift module and larval module (*Dagestad et al.*, 2018). There are a number of advantages in this model. For example, it can simulate a massive number (millions) of particles on a laptop. OpenDrift can run on various operating systems including Windows, Mac and Linux. Another advantage of OpenDrift is that there is a Graphical User Interface which is especially convenient for those who have minimal or no Python experience. The most helpful function to me when using OpenDrift is that it can read forcing data (e.g. wind, waves and currents) from any possible source without any modification, or conversion to readable format by OpenDrift.

In my research I used the OpenDrift model to simulate marine plastics drifting from Mekong deltas to the South China Sea and its surrounding waters. To be able to work flexibly and to save my time and resources for my laptop, I installed OpenDrift on HPC of Meteorological Institute named PPI. For the simulations, the OpenDrift requires winds and ocean currents. Wind data is downloaded from CMEMS (see section 3.2.2). The ocean current is simulated by ROMS for the South China Sea (see section 3.1.3). For the area outside the ROMS domain, CMEMS ocean currents are used (see section 3.2.1). ROMS domain and CMEMS current domain can be seen in figures A2 and A3.

The Mekong River has six to eight mouths, and I divided them into four sources (see green stars in figure A12) of plastics based on their geographical locations. The amount of particles are released at each source in proportion to its maximum discharge rate. Specifically, in my simulations I use 100,000 plastic particles, in which Dinh An - Tran De is 42,000, Co Chien is 24000, Ham Luong is 8000, and Dai Tieu is 26000.

In this thesis, I often use the term 'seasonal' to refer to the short term, 3 months, summer and winter, and use the term 'long term' to refer to 15 months. To examine how plastics drift in the short terms, I release the particles evenly over 90 days from 1/6/2020 in the summer, and from 1/12/2020 in the winter. In addition, *Haberstroh et al.* (2021) show that plastic waste in Mekong river mostly floats on the surface and drifts to the sea during the flood season. Therefore, I assume plastics drift to the sea in the first half of the flood season, or from June to October. To examine how plastics drift in the long term, 15 months, I release the particles evenly over 150 days from 1/6/2020, or from June to October, and let them drift in 10 months.

In general, the simulations take into account the ocean currents, wind drift (2% of the wind), high frequency river water (daily), constant positive terminal velocity (0.01m/s upward), vertical diffusivity ($0.02 m^2/s$). The stranding of plastics by default is not taken into account. However, when considering the influence of each factor, it will be changed and will be noted clearly.

3.1.3 Vietnam ROMS3D

The ocean currents are simulated using Vietnam ROMS 3D developed by MET Norway in collaboration with Vietnam national center for hydro-meteorological forecasting (NCHMF). The grid is set up specifically for Vietnam's waters (fig. A14), where the resolution at the coast of Vietnam is 1 - 3km. The areas far from the coast of Vietnam like the Philippines is quite coarse, 5 - 7km. The water column is divided into 20 levels. This model uses several inputs, oceanic conditions, atmospheric conditions, river discharge rate and tides. I use oceanic conditions downloaded from CMEMS. The data then is converted into readable format and used as the initial and boundary

conditions for ROMS (see section 3.2.3). Atmospheric conditions from ECMWF provided by MET are converted into readable format and then used as the forces for the ROMS model (see section 3.2.4). Daily river discharge rates at Mekong estuaries are from the Mike 11 model operated at VNMHA and the discharge rates at other major rivers around the South China Sea are from the European Flood Awareness System (EFAS). The reason for the two different sources is that the discharge rates from EFAS are available for all rivers but low accuracy while that from VNMHA is more accurate but only available at Mekong estuaries (see sections 3.2.5 and 3.2.6). The tides in the ROMS model are taken from the OSU TPXO Tide model (*Egbert and Erofeeva*, 2002) with 13 tidal constituents, which are M2, S2, N2, K2, K1, O1, P1, Q1, M4, MS4, MN4, MM and MF. In this study, I downloaded and processed atmospheric data, oceanic conditions and river discharge rates from VNMHA and EFAS. However, the tidal constituents are already available in the ROMS model.

I extracted the output variables of the ROMS model with a time step of 1h. They include ocean currents, water level, temperature and salinity. The currents are used for plastic simulations by OpenDrift. Whereas, water level, temperature and salinity are used for comparison with the observations.

3.2 Data

3.2.1 CMEMS current for OpenDrift

CMEMS stands for Copernicus Marine Environment Monitoring Service (or the Copernicus Marine Service). It is the marine part of the Copernicus Programme of the European Union, and provides free, regular and systematic forecast and reanalyses on oceans on global and regional scales. In my study, I use surface current (-0.47m) for the area beyond the South China Sea (or outside the ROMS domain). There is a wide range of velocity datasets. For my study area, there are 14 datasets. I choose the latest, highest resolution one (Global Ocean 1/12° Physics Analysis and Forecast updated Daily), which is updated daily. This dataset provides 3D data from 2019 to present and next 10 days forecast with spatial resolution is 0.083° in longitude and latitude over the global ocean. It also has a variety of data including temperature, sea surface height, current and salinity. They can also be extracted at different time steps for example hourly, every three hours, daily and monthly. For this purpose I used daily velocity data.

3.2.2 CMEMS wind for OpenDrift

Although I can use ECMWF wind (section 3.2.4) for plastic simulations, I decided to use this CMEMS wind because it is reanalyzed data combined with observations. There are 3 products that can suit my study with different time steps: hourly, every 6 hours, and monthly. Since the wind field is relatively stable in some hours and the limited size of data that can be loaded at a time, time step of 6 hours (or the product WIND_GLO_WIND_L4_REP_OBSERVATIONS_012_006) is the most suitable for my research. This is re-analysed data, and also makes use of the remotely sensed surface winds derived from scatterometers and radiometers. The spatial resolution is 0.25° in longitude and latitude over the global ocean.

3.2.3 CMEMS oceanic data for ROMS

I use oceanic conditions downloaded from CMEMS as initial and boundary conditions for the ROMS model. This data set includes sea surface height, salinity, temperature and currents. The sea surface height is 2D and the rest is 3D. These variables are then renamed, their units are converted, and written in readable format by ROMS. I use the same product as described in CMEMS currents for OpenDrift (or the Global Ocean 1/12° Physics Analysis and Forecast updated Daily). The difference is that the data for OpenDrift is the surface current only, while the data for ROMS takes more parameters (3D current, sea surface height, salinity and temperature). CMEMS limits the size of data (1GB) to be loaded at a time, I had to do multiple downloads and then combine them into one file.

3.2.4 ECMWF atmospheric data for ROMS

Atmospheric forces act on the sea surface, and it changes the dynamics process of the sea. In the ROMS model, atmospheric force is one of the most important inputs. In the ROMS simulations, I use atmospheric conditions from ECMWF with a spatial resolution of 0.125° in longitude and latitude, and the time step is very three hours. This data is provided by MET. The data includes wind at 10 meter, sea level pressure, temperature at 2 meter, total cloud cover, precipitation rate and dew-point temperature at 2 meter. These variables are then renamed, used to calculate new variables, their units are converted, and written in readable format by ROMS.

3.2.5 River discharge from EFAS for ROMS

EFAS is one of two river discharge sources that I used as river input for ROMS model. This dataset is downloaded from https://cds.climate.copernicus.eu/. The data is represented as a grid across the whole globe with each grid node corresponding discharge rates at one location. Grid nodes on land contain realistic values, while those on sea/oceans contain empty values. I define a river as a collection of points of high discharge rate. For example, in figure 2.1, the rivers in red are the collection of points with the maximum of 10-year mean over 2000 m^3/s. The accuracy is relatively good for the total discharge of big rivers, see figures 3.4 and 3.5. However, when flowing to smaller rivers, the accuracy is significantly reduced in sub-rivers, see figures A15 and A16. Perhaps this is because global model is quite accurate at large scales but not at small scales. For the above reason and for the most realistic ROMS simulations possible, there is a need for a better data source if possible.

3.2.6 River discharge from VNMHA for ROMS

The Mike 11 model has been developed and used in Vietnam for more than 20 years. During this time period, the data is updated annually including cross-sectional data, observations and parameters in the model. After comparing this data with the observations, it shows that this data is clearly better than the European Flood Awareness

System, see more at A15 and 3.6. I decided to use this Mike 11 data where possible, specifically the Mekong estuaries. The discharge rate details of these estuaries are shown in figure A13.

3.2.7 Observations

There are many stations on the rivers and on the sea. These stations usually measure temperature, salinity, water level, discharge, sediment, water quality and biochemical factors. One station focuses on one or more types of data, one parameter can have one or more observation frequencies, and the duration of observations vary between stations. However, there are some general trends, including the increase in frequency of observation, the number of stations, the number of observed variables and quality of observation. For example, in recent decades the frequency of observations has increased from twice per day to four times per day, or from four times per day to hourly. There are more observed variables at one station, and more stations than it was. The quality of observations also increase as high-quality measuring instruments replace manual work. The data in this study is from my former colleagues at VNMHA and it is free of charge for scientific research purposes. These data are usually recorded in local format, for example, the time, units, datum and language. Therefore, although the observations are officially available for everyone, it is not published and unreadable for a non-Vietnamese. For hydrological stations, I use observed discharge rates on the Mekong river and the Red river to validate discharge rate from VNMHA (local model Mike 11) and EFAS (global model). These two rivers are the 1st and 2nd largest rivers in Vietnam, and the 1st and 3rd largest rivers in the South China Sea. For marine stations, I use water level, temperature and salinity at Vung Tau station (see figure A12), the closest station to the Mekong River. This is one of the oldest stations with the highest frequency of observation in Vietnam.

3.3 Model validation

3.3.1 OpenDrift

As mentioned earlier, OpenDrift is a common framework for ocean trajectory modeling, and it is designed to accommodate various drift simulations. Several modules have already been developed, including oil drift, search and rescue, fish eggs, chemicals, plastics drift. This model has been used in many studies as well as scientific articles[1]. However, not all modules have been tested. Here I give two examples of model validation for OpenOil in two oil spills. One is in the North Sea in 2019. The other one is in the Northern Gulf of Mexico in 2010.

Brekke et al. (2021) used the OpenDrift to simulate the oil spill in the North Sea in 2019. They use module OpenOil to simulate oil drift (trajectories, dynamics and evolution of the spills and slick extent) with various configurations of wind, wave and current. The predicted results were compared with observations from optical instruments with different detection capabilities versus multifrequency PolSAR acquired by

[1] https://opendrift.github.io/references.html

Deutsches Zentrum für Luft-und Raumfahrt F-SAR. The comparisons show that it is possible to obtain good agreement between the model and observations. Specifically, when using the best available data from in situ data and forecast models, good agreement between observed and predicted positions was seen. Also, a fair agreement was seen using only numerical forecast data.

Hole et al. (2019) reproduced the Deepwater Horizon oil spill. In this study they used Metocean data from the data-assimilative GoM-HYCOM 1/50° ocean model with realistic daily river input and products of wind and wave from ECMWF. The initial condition is the satellite observations of the surface oil patch. There is a good agreement between the model and satellite observations after simulating the surface oil patch drift for 7–8 days. Also, the simulations show that the outcome is robust regarding the choice of parameterization.

3.3.2 ROMS

There are many stations in the South China Sea, and three of them near the Mekong mouths, Vung Tau (20-50km) (see figure A12), Con Dao (120km) and Phu Quy (250km). These stations observe water level, salinity and surface temperature. In this section, I use observations from Vung Tau station, the closest station, for the validation of ROMS.

Water level

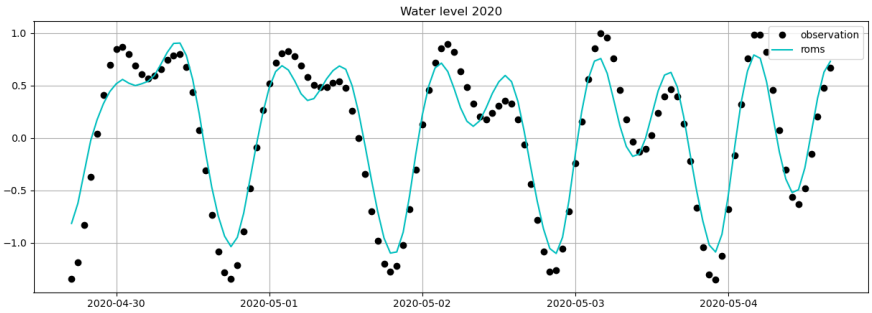

Figure 3.1: Compare ROMS (water level) with observation

This figure 3.1 shows a comparison between the observed water level at Vung Tau station and the ROMS model for the five days from April 29 to May 5, 2020. The black points are the observation, while the blue line is the model data. Although both observation and model data are about a year long, I extracted only 5 days. The observed data is hourly, in cm and compared with its own datum. Meanwhile, the roms model data is also hourly, in meter and compared with the geoid surface. These two data were then converted to the same unit of meter and compared with its mean. Overall, the comparison shows that there is a good match between ROMS model and observations.

Temperature

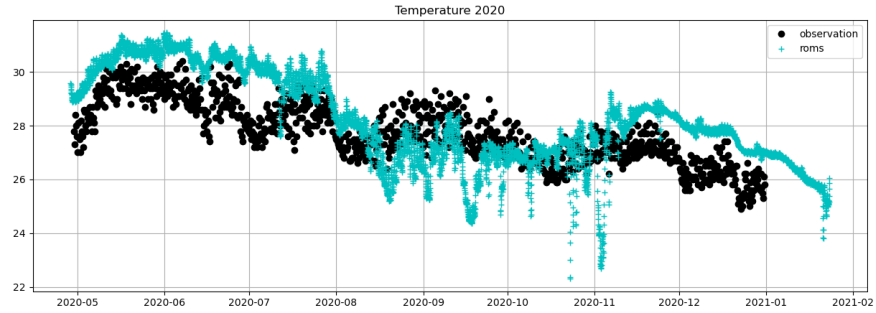

Figure 3.2: Compare temperature with observation

This figure 3.2 shows a comparison between the observed temperature in Celsius at Vung Tau station and the ROMS model from May to December 2020. The black points are the observations, while the blue point is the model data. The frequency of observed data is every 6 hours, while the ROMS model data is hourly. This result shows that although there is a clear decrease in temperature from the summer (May) to the winter (December), a match between ROMS model and the observations is seen. This is probably because temperature extracted from the model is potential temperature in the uppermost layer while the observations are the temperature right at the surface.

Salinity

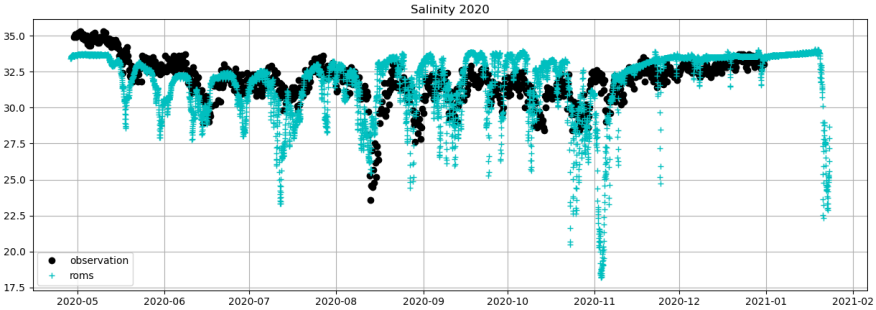

Figure 3.3: Compare salt with observation

This figure 3.3 shows a comparison between the observed salinity in psu at Vung Tau station and the ROMS model from May to December 2020. The black points are the observations, while the blue points are the model data. The frequency of observed data is every 6 hours, while the ROMS model data is hourly. This result shows that there is a moderate match between ROMS model and the observations. The difference might be because the salinity extracted from the model is in the uppermost layer while the observations are right at the surface, and it is easily affected by fresh water from the river.

3.3.3 River discharge rates

Global model from EFAS

Compare EFAS with observations on the Mekong River

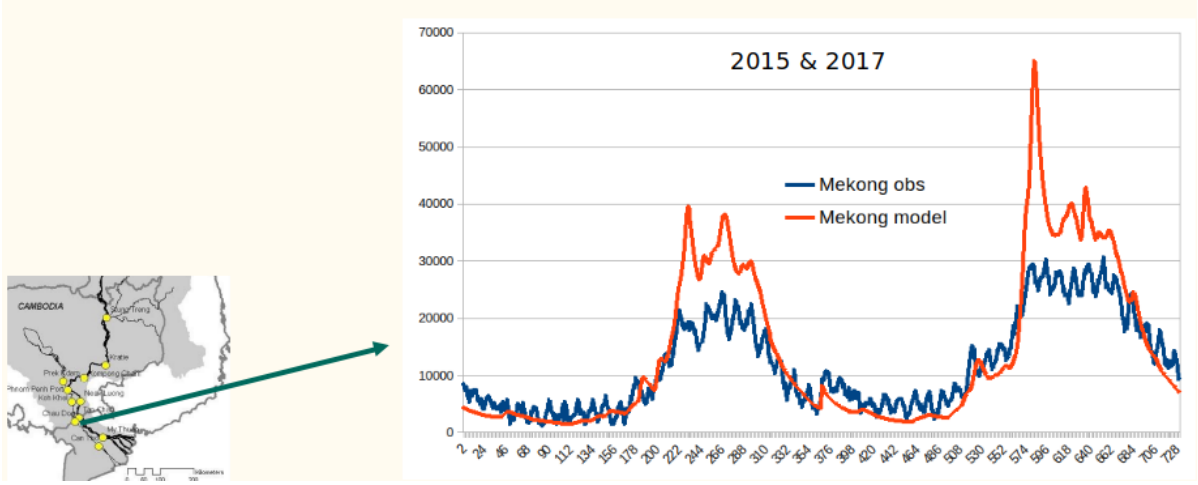

Figure 3.4: Compare EFAS with observations in Mekong River

This figure 3.4 compares the observed discharge rate (m³/s) in blue with the global model data from EFAS in red on the Mekong River at the border between Vietnam and Cambodia, about 400 kilometers from the shore in 2015 and 2017. This result shows that the model gives relatively good data most of the time except the peak of the flood.

Compare EFAS with observations on the Red River

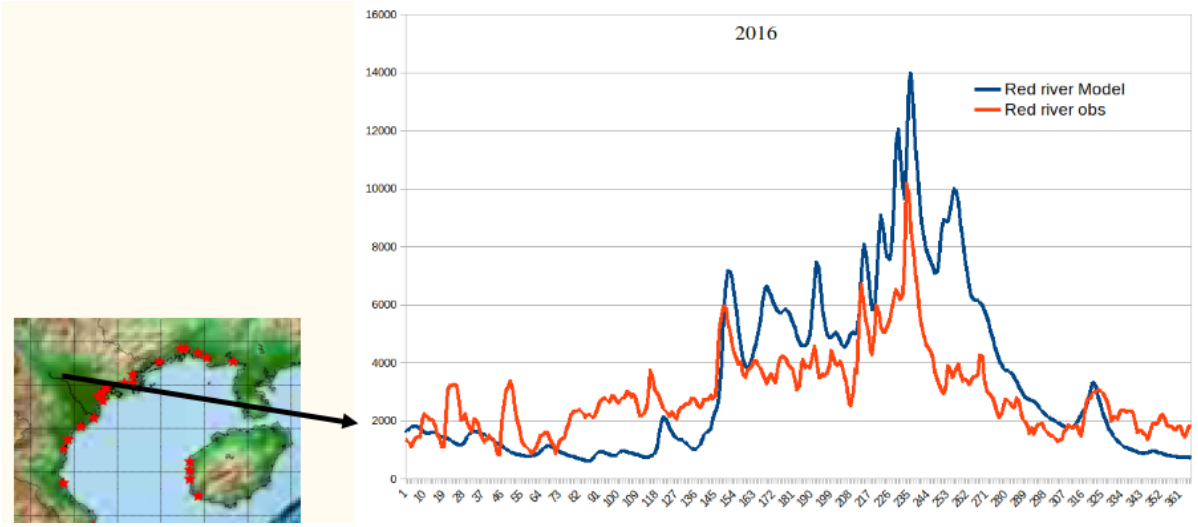

Figure 3.5: Compare EFAS with observations in Red River

This figure 3.5 compares the observed discharge rate (m³/s) in red with the global model data from EFAS in blue on the Red River in Hanoi, about 100 kilometers from shore, in 2016. This result shows that the model can somewhat reflects the flood cycle.

The above results are probably relatively good. However, this is for the main stream (the whole river). When moving to the sub-rivers the comparison between the observa-

tions and model is very poor, see more in the figures A15 and A16. Therefore, there is a need for a better data set if possible.

Mike 11 from VNMHA

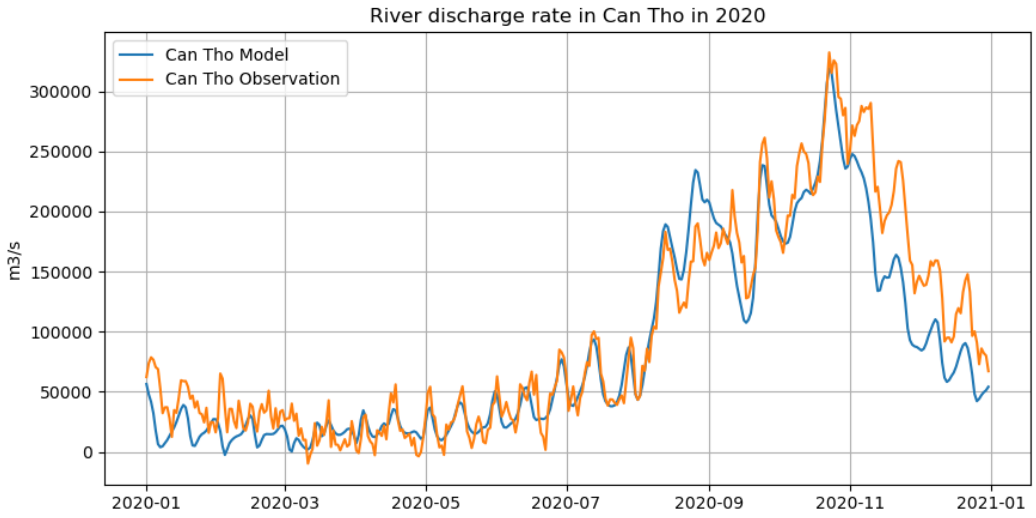

Figure 3.6: Mike 11 and observations in Can Tho, its location: A12

This figure 3.6 compares the observed discharge rate (m^3/s) in orange with the Mike 11 model from VNMHA in blue at Can Tho (its location: A12), one of the sub-rivers of the Mekong river, about 90 kilometers from shore, in 2020. This result shows a very good agreement between model and observation. However, this data is only available for the Mekong estuaries. Therefore, in ROMS, this data is used for Mekong mouths, while data from EFAS is used for other river mouths.

Chapter 4

RESULTS

4.1 Plastics drift in the summer

In the seasonal drifts (sections 4.1 & 4.2) and long term drift (section 4.3), the simulations use ROMS data as described in section 3.1.3, and the settings in OpenDrift are described in section 3.1.2. The simulations take into account the ocean currents, wind drift (2% of the wind), high frequency river runoff (daily), constant positive terminal velocity (0.01m/s), vertical diffusivity (0.02m^2/s). The stranding of plastics is not taken into account.

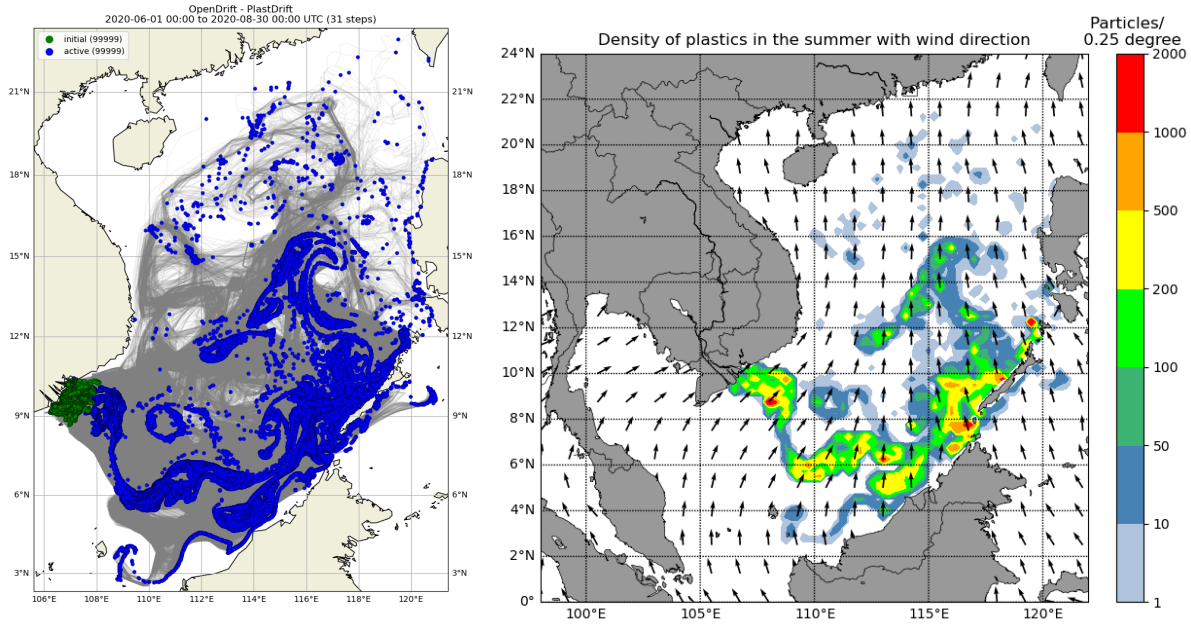

(a) Trajectory *(b) Density*

Figure 4.1: Plastics drift in the summer

Fig. 4.1 shows trajectory (map a) and density (map b) of 100000 plastic particles over the three summer months from 1/6/2020. The particles are released evenly during this three-month period. The whole drifting can be found on youtube[1]. In map a,

[1] https://youtu.be/h02kSWJkPA0 : Plastics drift in the summer

the green particles are the starting positions, the grey lines are the trajectories of the particles, and the blue particles are the final positions. In general, particles drift in two main directions, east and northeast with a large number of particles towards the western coast of Malaysia and the Philippine. Whereas, map b represents the density of plastics at final locations in the number of particles per 0.25 square degree. It can be seen that the particles are concentrated mainly in the area off the Mekong River and the area between the southern Philippines and northern Malaysia. The highest density is up to 1000 - 2000 particles per 0.25 square degrees.

4.2 Plastic drift in the winter

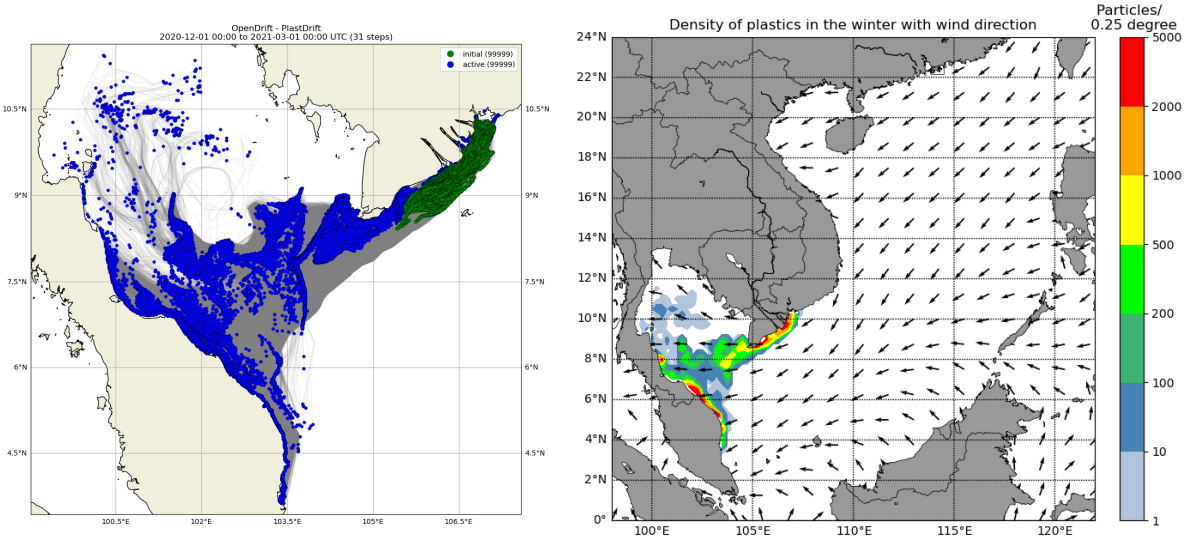

(a) Trajectory *(b) Density*

Figure 4.2: Plastics drift in the winter

Figure 4.2 shows trajectory (map a) and density (map b) of 100000 plastic particles over the three winter months from 1/12/2020. The particles are released evenly during this three-month period. The whole drifting can be found on youtube[2]. In map a, the green particles are the starting positions, the grey lines are the trajectories of the particles, and the blue particles are the final positions. In general, particles drift to the southwest direction. A large number of the particles drift the coast of Thailand and Malaysia. Whereas, map b represents the density of plastics at final locations in the number of particles per 0.25 square degree. We can see that the particles are concentrated mainly around the Mekong deltas and the area between Thailand and Malaysia. The density of particles is up to 2000 - 5000 particles.

[2]https://youtu.be/2ZTg5wW8E54 : Plastics drift in the winter

4.3 Plastic drift in 15 months

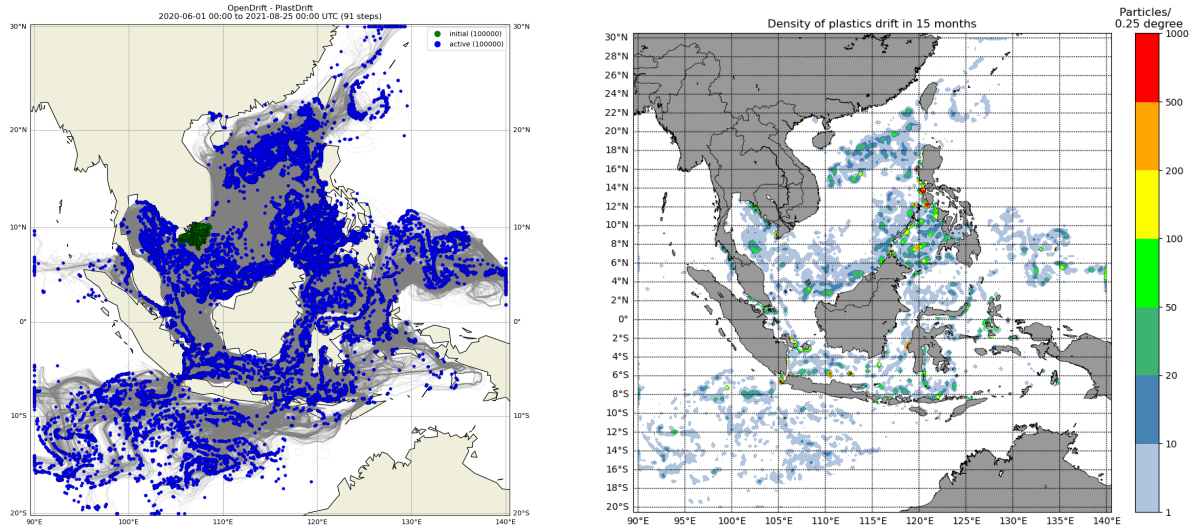

(a) Trajectory *(b) Density*

Figure 4.3: Plastics drift in 15 months

Figure 4.3 shows trajectory (map a) and density (map b) of 100000 plastic particles over 15 months from 1/6/2020. The particles are released evenly during the first five months from June to October. In map a, the green particles are the starting positions, the grey lines are the trajectories of the particles, and the blue particles are the final positions. In general, after 15 months the plastic particles drift on most of the seas and straits in Southeast Asia. Whereas, map b represents the density of plastics at final locations in the number of particles per 0.25 square degree. It can be seen that a large number of marine plastics enter the Sulu Sea (Philippines) and its vicinity with some locations up to over 500, followed by the Java Sea (Indonesia) and its vicinity with some locations up to over 200. There is still many particles left in the South China Sea, and a small amount drifts to the Indian and Pacific oceans.

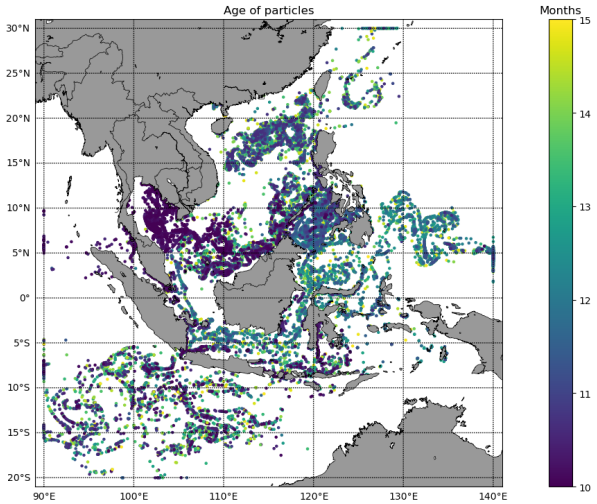

Figure 4.4: Plastic drift in 15 months with age

Another way to analyze the data is to look at the age of the particles. Figure 4.4 represents the age of the particles in months. In which, the yellow and green particles are released in the summer, and the blues and purples are those released in the fall. From the figure we can see that the yellows and greens are seen in all areas, for example, the South China Sea, the Sulu Sea, the Java Sea, the Indian and Pacific Oceans. Meanwhile, blue and purple particles appear mainly in the southern seas, including the south of the SCS, the Malacca Strait, Java Sea and Indian Ocean. The whole drifting can be found on youtube[3].

The above simulation does not take into account the stranding of plastics. It means when a plastic particle hits the coast, it would stay temporarily on the coast, and return to the sea under favorable conditions. In reality, the physical processes are more complex, for example some stranded particles would stay at the coast indefinitely. Therefore, the next section will consider the stranding of marine plastics.

4.4 The influence of stranding on plastics drift

The previous sections do not take into account the stranding of plastics. This section will examine the effect of stranding on the distribution of marine plastics. It means when the plastic particles hit the coast, they would be stranded and stay there indefinitely. In this simulation, the settings are the same as those in the long-term simulation (section 4.3). The only difference is that the particles would be deactivated (stay indefinitely) when hitting the coast.

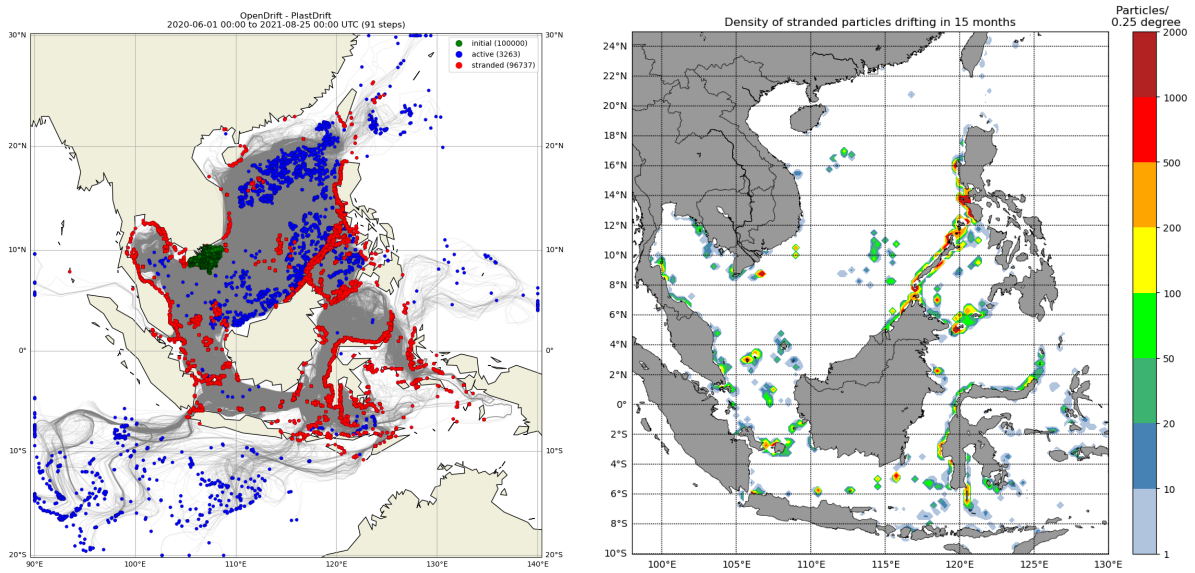

(a) Trajectory *(b) Density*

Figure 4.5: Plastic drift in 15 months with stranded mode

Figure 4.5 shows effect of stranding on the distribution marine plastics. In the map a, the green particles are the starting positions, the grey lines are the trajectories of the particles, the red particles are the stranded particles, and the blue particles are the final

[3]https://youtu.be/G9jyyxy5px8 : Plastics drift in 15 months

positions of the active particles. This result shows that after 15 months, around 97% of the particles are stranded, 2% continues to float in the SCS, the remaining 1% drifts to the Indian and Pacific Oceans, and the average travelling time of the stranded particles is 3.7 months. Whereas, map b represents the density of plastics at final locations in the number of particles per 0.25 square degree. The density map shows that a great number of the particles are trapped in the western coast of the Philippines. The density at some locations can be up to 2000 particles.

4.5 The influence of rivers on plastics drift

The purpose of this section is to show how strong rivers can affect the trajectories of particles in both the short and long term. To do this, I turned off rivers in ROMS (settings are in section 3.1.3 but no rivers) then re-run the ROMS model and OpenDrift. The settings in OpenDrift are in sections 4.1 and 4.3. The results are then compared with the results in sections 4.1 and 4.3. In other words, I examine the influence of rivers on plastics drift by comparing two simulations with and without river water in both short term and long term. This is similar to the model experiments carried by *Hole et al.* (2019) to study the effect of the Mississippi river on the Deepwater Horizon oil spill.

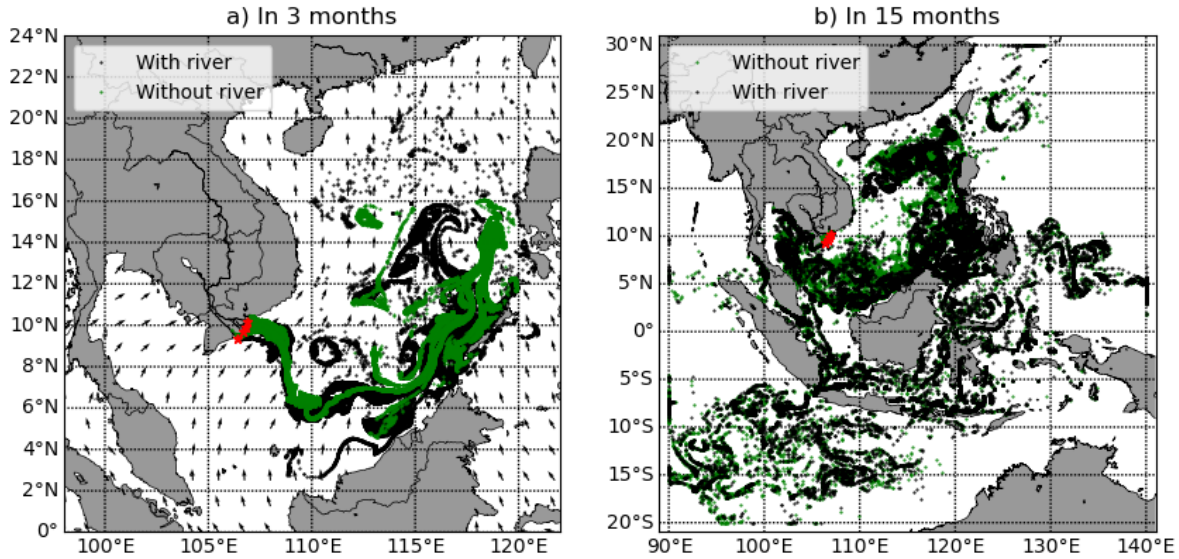

Figure 4.6: The influence of Mekong river on marine plastics

Figure 4.6 shows the influence of the Mekong River on the trajectory of marine plastics. The black and green colors represents the final locations of plastic particles in scenarios with river turned on and off, respectively. Figure (a) shows simulations of three months (short term), while figure (b) shows simulation of 15 months (long term). We can clearly see that in the short term, the greens is less dispersed than blacks. In other words, river water plays the role of dispersing marine plastics. However, in the long term, the effect of river water on the plastic drift is unclear with a similarity between the two scenarios in all seas and oceans.

4.6 The influence of river frequency on plastics drift

In this section the purpose is to examine how the frequency of river water can affect the trajectory of marine plastics in both short and long terms. To do this, I used a lower river frequency (the average in two weeks) in ROMS (settings are in section 3.1.3 but with low river frequency) then re-run the ROMS model and OpenDrift. The settings in OpenDrift are in sections 4.1 and 4.3. The results are then compared with the results in sections 4.1 and 4.3. In other words, I examine the influence of river frequency by comparing two scenarios with high and low river frequencies in both short and long terms.

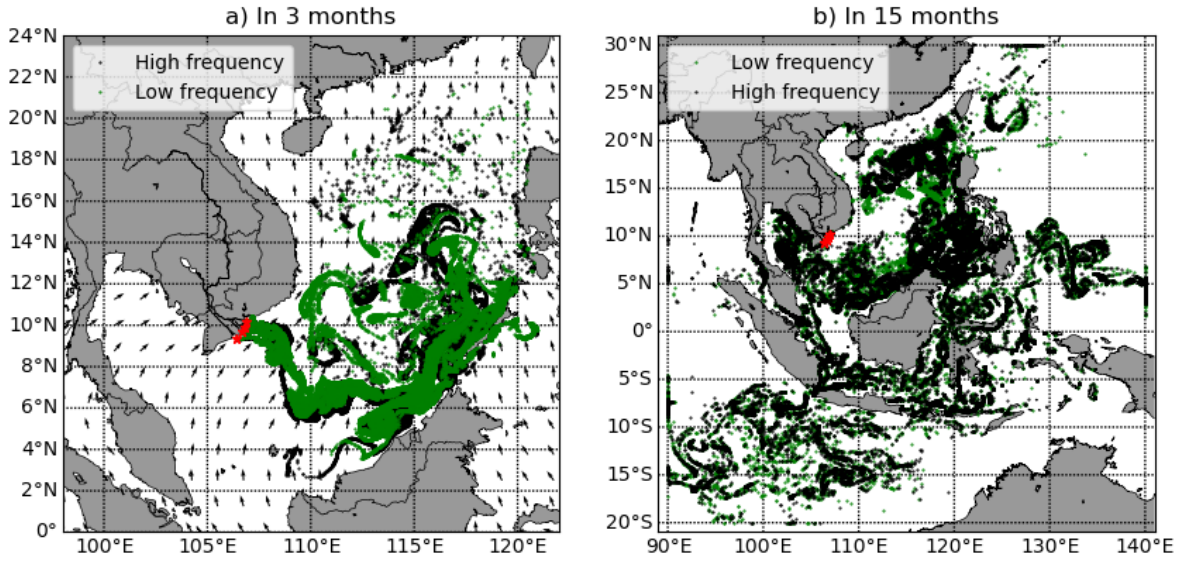

Figure 4.7: The influence of river data frequency on marine plastics

Figure 4.7 shows the influence of river frequency on the trajectory of marine plastics. The black and green particles represents the final locations of plastic particles in scenarios with high and low frequency of river data. High frequency means daily data while low frequency means 14-day average data. Figure 4.7 (a) shows simulations of three months (short term), while figure 4.7 (b) shows simulations of 15 months (long term). Overall, in the short term the result shows that there is a difference in the dispersal of the particles between the two scenarios. However, there is no general trend of how different the dispersions are. The 15 month simulations show a similarity between the two scenarios in all seas, straits and oceans, or the effect of river frequency on the plastics drift is negligible.

4.7 The influence of wind drift current on plastics drift

Wind drift plays a significant role in the accuracy of predicting trajectories of objects at sea (*van der Mheen et al.*, 2020). Therefore, the purpose of this section is to examine how wind drift (Stokes drifts + wind shear) can affect the trajectory of marine plastics. In this section, I used ROMS output as described in section 3.1.3. The settings in OpenDrift are described in section 3.1.2 but wind drift is turned off (or wind drift

factor = 0% of the wind). The results are then compared with the results in sections 4.1, 4.2 and 4.3. In other words, I examine the influence of wind drift by comparing two scenarios with and without wind drift in both short and long terms.

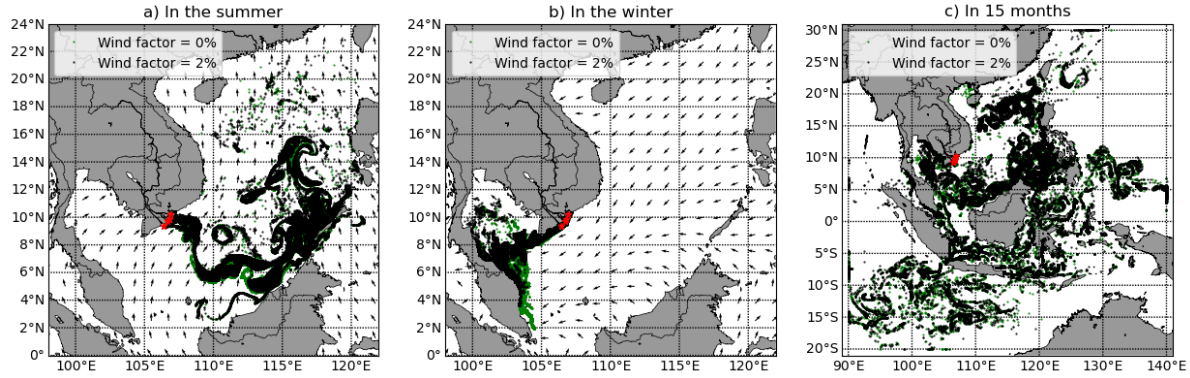

Figure 4.8: The influence of wind drift on marine plastics

Figure 4.8 shows the influence of wind drift on the trajectory of marine plastics. The black and green colors represents the final locations of plastic particles in scenarios with wind drift turned on (wind drift factor = 2%) and off (wind drift factor = 0%), respectively. Figures 4.8a and 4.8b show simulations of three months (short term), while figure 4.8c shows simulations of 15 months (long term). We can clearly see that in the summer the influence of wind drift is negligible while in the winter wind drives the plastics to the west. The 15-month figure shows a similarity between the two scenarios in all seas, straits and oceans, or the effect of wind drift on the plastics drift is also negligible.

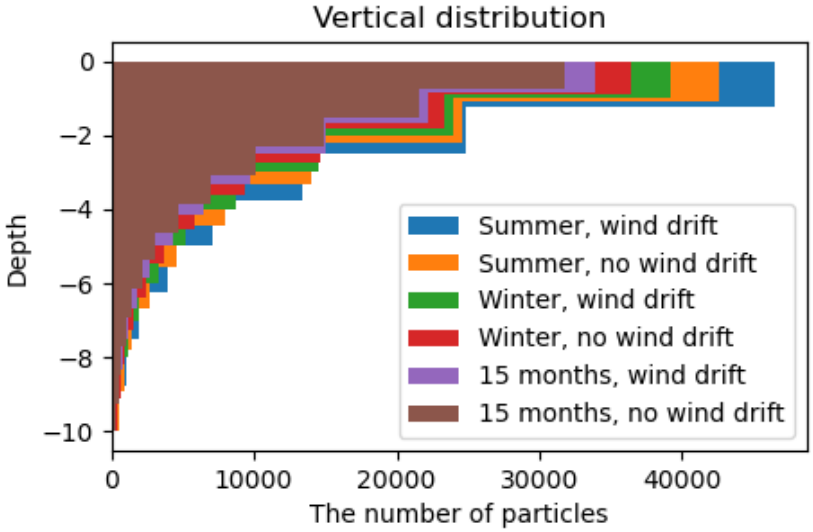

Figure 4.9: The histogram of vertical positions in all simulations

This figure 4.9 shows the vertical distributions of particles in all simulations. Although the distributions seem different, they actually have an almost identical distribution. They are divided by different number of bins for the convenience of readers. In general, most particles in the depth between 0 and 5 meter.

4.8 The influence of vertical mixing on plastics drift

The vertical mixing also can play a role in the distribution of buoyant particles (*Kooi et al.*, 2016; *Kukulka et al.*, 2012; *Röhrs et al.*, 2018). Therefore, the purpose of this section is to examine how vertical mixing (vertical diffusivity) can affect the trajectory of marine plastics. In this section, I used ROMS output as described in section 3.1.3. The settings in OpenDrift are described in section 3.1.2 but vertical mixing is turned off (or no vertical diffusivity). It is worth mentioning that the vertical eddy diffusivity can be either extracted from ROMS or activated in the OpenDrift. In this study I used default value of 0.02 m^2/s in the OpenDrift model. The results are then compared with the results in sections 4.1 and 4.3. In other words, I examine the influence of vertical mixing by comparing two scenarios with and without vertical mixing both short term and long terms.

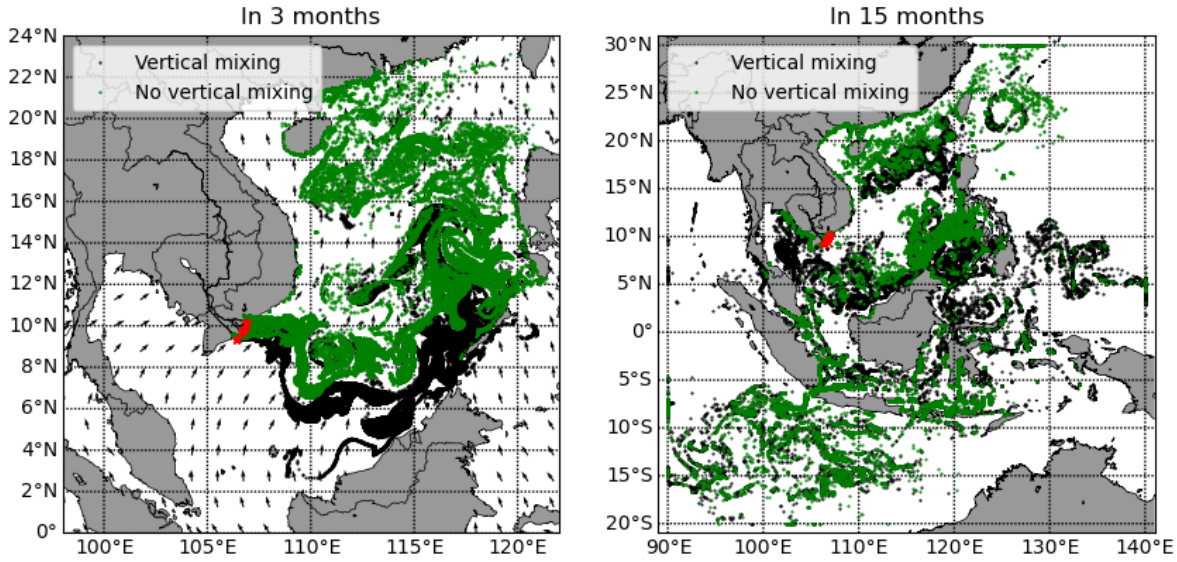

Figure 4.10: The influence of vertical mixing on marine platics

Figure 4.10 shows the influence of vertical mixing on the trajectories of marine plastics. The black and green colors represents the final locations of plastic particles in scenarios with vertical mixing turned on and off, respectively. Figure 4.10a shows simulations of three months (the animation driftings without the influence of vertical mixing can be found on youtube [4] [5] [6]), while figure 4.10b shows simulations of 15 months (the animation drifting without the influence of vertical mixing can be found on youtube[7]). We can clearly see that in the short term the influence of vertical mixing is very significant with many green particles drifting far to the north, while black particles are concentrated in the middle of the sea. Specifically, the average latitudes of the black and green particles are 8.5°N and 11.8°N, respectively. In other words, without vertical mixing the particles would drift 360 km further to the north. Whereas, the 15-month figure shows the effect of vertical mixing decreases over time. Although the difference

[4] https://youtube.com/shorts/rXe9_g5yUkA : drifting in three months
[5] https://youtube.com/shorts/zsfUD9Z_t9I : drifting in three months with ocean current background
[6] https://youtube.com/shorts/39yVq0DUw_o : drifting in three months with wind background
[7] https://youtu.be/3ZntxFP40Bw : drifting in 15 months

between the two scenarios is still visible, it is less distinct than that in the short term. The average latitudes of the black and green particles in the long term simulations are 6°N and 8°N, respectively. To put it another way, in the long term simulations, without vertical mixing the particles would drift 210 km further to the north.

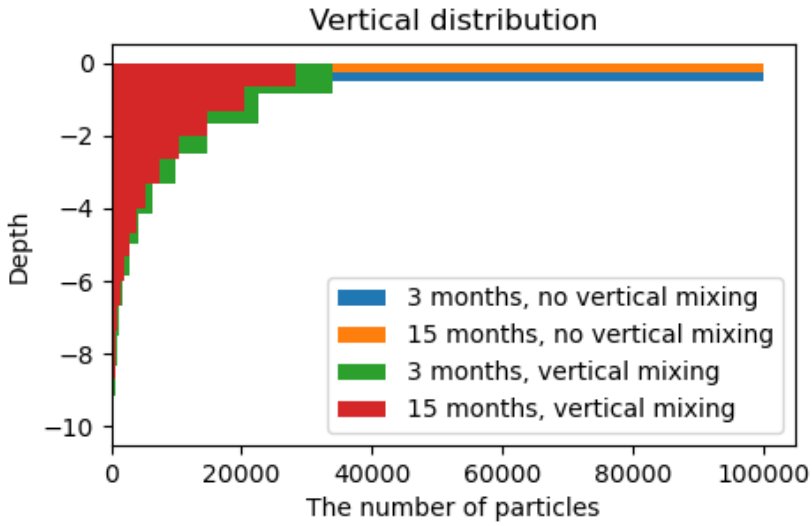

Figure 4.11: The vertical distribution of plastic particles in all simulations

Figure 4.11 shows the distributions of particles in vertical positions in all simulations. In general, we can see a huge difference between scenarios with and without vertical mixing. In scenarios with vertical mixing, most particles in the depth between 0 and 5 meter, a few can reach 10m. In comparison, in the scenarios without vertical mixing, all the particles stay at the surface or 0m.

4.9 The influence of biofouling on plastics drift

Biofouling is also one of the processes that deposit microplastics (*Kaiser et al.*, 2017; *Lobelle et al.*, 2021; *Van Sebille et al.*, 2020). Therefore, the purpose of this section is to examine how biofouling (sinking) can affect the drifting of marine plastics. The settings of ROMS are described in section 3.1.3. The settings in OpenDrift are described in section 3.1.2 but the terminal velocities are fixed at 1, 2 and 5 meters/day (m/d) and downward. I also assume that if a particle hits the bottom, it would be deactivated. Finally, the plastics take weeks to months to be biofouled; however, in this study, I assume that the plastic particles are already bio-fouled as they are released on the sea.

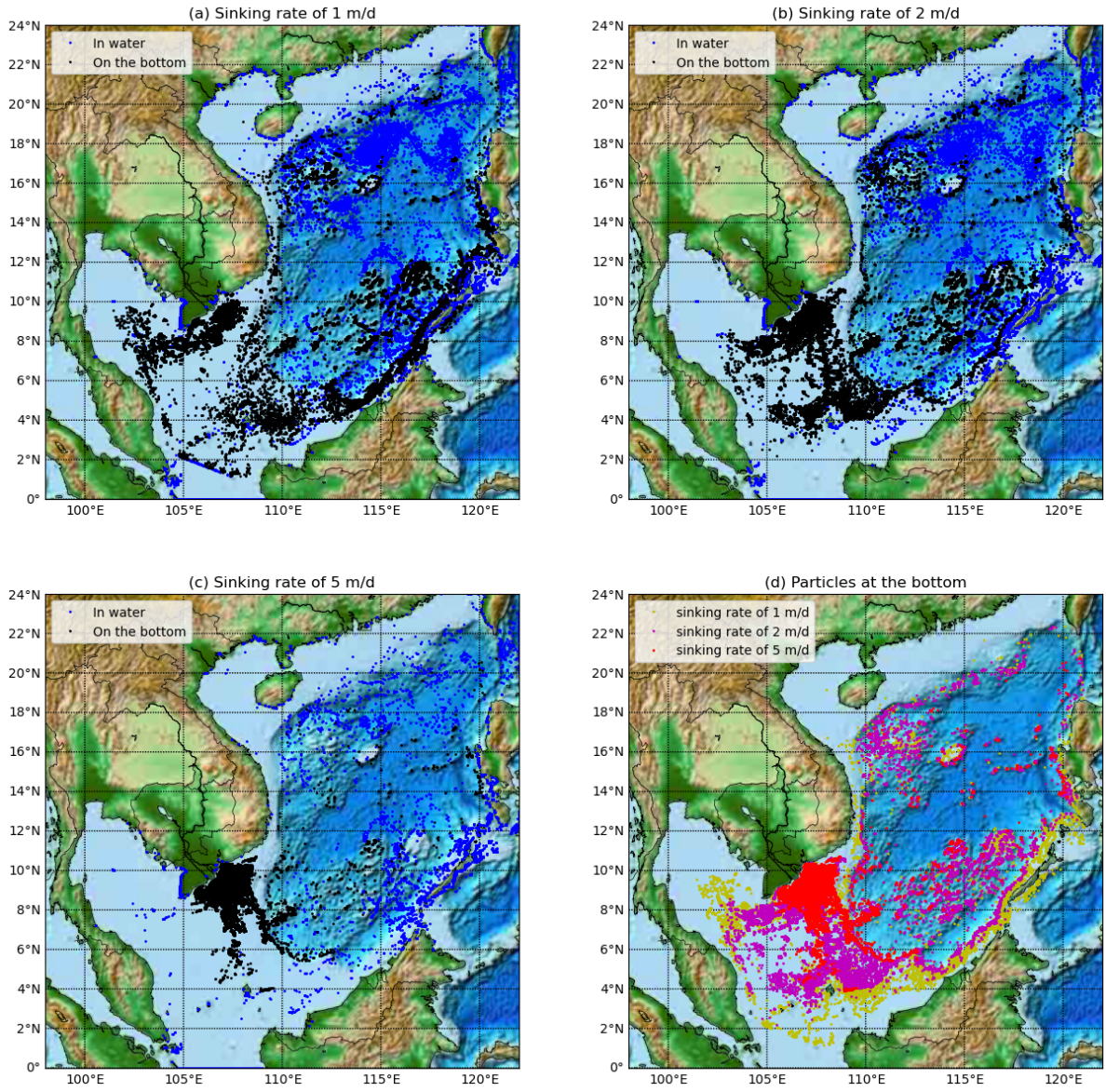

Figure 4.12: The influence of biofouling on the trajectory of marine plastics in 15 months

These simulations (figure 4.12) represent the influence of biofouling on the trajectory of marine plastics. In the first three maps a, b and c, the blue (active) and black (inactive) colors represents the final locations of particles suspended in seawater and stranded on the sea floor in scenarios with sinking rate of 1, 2 and 5 m/d. The animations of these simulations can be found on youtube [8] [9] [10] [11] [12] [13]. The last map (d) shows final positions of the particles stranded on the sea floor in all three simulations with sinking rate of 1, 2 and 5 m/d. These particles are in yellow, purple and red, respectively.

There are some obvious results we can notice here. The particles on the bottom

[8] https://youtube.com/shorts/JzEFYd4E4Jw : Plastics drift with terminal velocity of 1 m/d
[9] https://youtu.be/MnXDdU6MwYw : Vertical distribution with terminal velocity of 1 m/d
[10] https://youtube.com/shorts/Jdb8PaFL4iE : Plastics drift with terminal velocity of 2 m/d
[11] https://youtu.be/3HMkh5RGUzE : Vertical distribution with terminal velocity of 2 m/d
[12] https://youtube.com/shorts/Yew3WEBeME4 : Plastics drift with terminal velocity of 5 m/d
[13] https://youtu.be/DhUd_5QyWms : Vertical distribution with terminal velocity of 5 m/d

are always those in shallow areas, typically the southern continental shelf of the sea, and the areas with large variations in depth such as the western coast of Palawan Island (Philippines), the Spratly and Paracel Islands. Blue (active) particles, are still suspended in deep water areas, and areas with large variations in depth. The details of the bathymetry can be seen in figure A17.

The map a with sinking rate of 1 m/d shows the blues are concentrated in the deep waters, mostly in the north of the sea. Meanwhile, the black particles are distributed mainly on the southern continental shelf of the South China Sea, and the western coast of the Philippines and Malaysia. In areas with great variation in depth, such as the Paracel and Spratly Islands, there is a relatively balanced presence of both blacks and blues.

In the map b with sinking rate of 2 m/d, there is a similarity to the 1 m/d simulation. However, it can be clearly seen that there are less blacks in the west of the Philippines and Malaysia, and more black ones in the southern continental shelf of the sea.

Map c with a much faster terminal velocity shows that the blues are much less in the deep waters. Meanwhile, the black particles are mainly distributed near the deltas of the Mekong river, mostly within two degrees or 220 km from the Mekong deltas.

The map d represents all particles on the bottom in all three scenarios. In this map the yellow, purple, and red particles are the final locations of particles in scenarios with sinking rate of 1, 2 and 5 m/d, respectively. They are also drawn in yellow, purple and red order. That means there might be some purple and red ones, which overlap the yellow ones. Similarly the red ones may overlap the purple ones. However, this map still gives us a general view of where the particles are most likely to sink, the southern continental shelf of the South China Sea.

Chapter 5

DISCUSSION

5.1 Seasonal and long term plastic drifts

The plastics drift in the summer indicates that the western coast of the Philippines and Malaysia is vulnerable to plastic pollution from the Mekong river with the density up to 1000 - 2000 particles per 0.25 square degrees. This is because the southwesterly monsoon in the summer pushes plastic particles from Mekong mouths to the east and the northeast of the sea. Most of the particles drift perpendicular to the shoreline within a few hundreds of kilometers from the Mekong deltas. This is the result of that the wind blows steadily over months and the wind is paralleled to the shore, consequently drives the particles perpendicular to the shoreline. It should be noted that the wind blowing during this period is not always stable in both speed and direction. The speed and direction can fluctuate during this time, as can be seen in figure A5.

The plastics drift in the winter shows that the south of Thailand and the Northwest of Malaysia are vulnerable to plastics from the Mekong river. This is because in the winter the northeasterly monsoon pushes the plastic particles to the southwest direction. In terms of density, the density of particles in the winter is much higher than that in the summer, with up to 2000 - 5000 particles. This is probably a result of the wind direction in combination with the shape of the shoreline.

In a field study on microplastics in the northwest Malaysia, *Khalik et al.* (2018) showed that the mean abundance of micro-plastics is 0.13-0.69 particles per liter (pcs/L). Although the authors know that Malaysia is one of the biggest contributors of marine plastics in Asia, they are not sure whether this amount is larger or smaller compared to other regions. They compared the value with other papers by *Qu et al.* (2018) and *Song et al.* (2015), but these papers give far different number due to very different approaches. For example, microplastics are classified as particles with a diameter of 0.001 to 1 mm (*Bermúdez and Swarzenski*, 2021). Whereas, *Khalik et al.* (2018) count only larger particles with a diameter of over 5mm. Perhaps this is why their results are far lower than the results of other authors, especially 0.68 to 6.44 pcs/L in Yantai-Qinzhou coastline area (*Qu et al.*, 2018) and 88 pcs/L in Jinhae Bay, Korea (*Song et al.*, 2015).

As mentioned above, since plastics are mostly released into the sea during the flood and the summer, the winter scenario is less realistic. However, it also shows that the difference in plastic drift between the two seasons is huge, one drifts to the Northeast and the other drifts to the Southwest.

Comparing the long term simulation with the short term simulations, it can be seen that within three months all the particles drift within the South China Sea. However, after 15 months, more than half of the particles are out of the sea, and many of them are on the two neighboring oceans. Figure 4.4 shows that the yellow and blue (summer) particles appear in most places and the purple and blue (autumn) ones mainly appear in southern areas. This is a result of that the yellow and green particles released in the summer has more time for dispersal on its way, drifting northward in the summer and southward in the winter. Also, the purple and blue ones were released in the autumn has less time to disperse, mostly drifting southward, and many of them are stuck in the Gulf of Thailand for a while.

It should be noted that the simulations in this section 5.1 take into account the ocean currents, wind drift, high frequency river water (daily), constant positive terminal velocity (0.01m/s), vertical mixing ($0.02m^2/s$). The stranding is not taken into these simulations, or when a plastic particle hits the shore, it is temporarily stranded and will return to the sea under favorable conditions.

5.2 The stranding of marine plastics

As shown in previous parts, the plastics are released in the summer and the fall, prevailing southwesterly winds push the particles from the Mekong River to the west of the Philippines. So this area is the hot spot of the stranded particles.

As we know, in practice, plastic waste is very diverse in shape and size. There are types that are easily stranded when going ashore. Sometimes plastics return to the sea under favorable conditions. The features of the shoreline also greatly influence the stranding and the return back to the sea, such as vegetation, sediments, rocks. Beach characteristics like steepness and sediment type could determine which particles get stranded (*Van Sebille et al.*, 2020). However, this knowledge has not been included in the OpenDrift model.

Probably, the stranding of plastics is one of the reasons why the estimates of the amount of plastics dumped into the seas and oceans are so much larger than the estimates of the amount of plastics actually in the oceans (*Van Sebille et al.*, 2020).

5.3 Rivers dispersing marine plastics

It is clear that the Mekong River disperses the plastic particles more efficiently in the short term. This is a result of that rivers generate eddies (*Cushman-Roisin*, 2011) that carry plastic particles or the mixing is more efficient. However, in the long term, the influence of the river on the trajectory of plastics is negligible. This is probably because the river flow is only strong enough to affect the areas around the rivers and for a limited time.

The comparison of simulations between high (daily) and low (two weeks) river frequencies shows that the frequency plays a role in dispersing the marine plastics in the short term. However there is no general trend of how different the dispersion is. In the long term the effect of river frequency on the plastics drift is negligible. The long term effect of river frequency is not surprising because I have already found that the influence of the river on the trajectory of plastics is negligible in the long term.

5.4 The importance of wind drift

The comparison of simulations between wind drift turned on (2%) and off (0%) indicates that the influence of wind drift on the trajectory of plastics is mainly in the winter. In comparison, in the summer and in the long term, this influence is negligible. There is some explanations for these results. Firstly, most of the particles below sea surface in between 0 and 5 meter depth, see 4.9. As a result, the impact of wind drift of several tens of centimeters has little effect on the particles. Secondly, as mentioned earlier, the wind in the winter is northeasterly and stronger at speed of 8-10 m/s, while in the summer the southwesterly wind is weaker with speed of 4-5 m/s. The wind drift is fixed at 2% of the wind, meaning that the wind drift in the winter is twice as strong as in the summer. Also, the currents in the area off the Mekong River (where plastics drift in the summer) with speed of 0.5-1.5 m/s are much stronger than the currents in the Gulf of Thailand (where plastics drift in the winter) with speed less than 0.3 m/s, see figure A9. In other words, the influence of wind drift on the trajectory of plastics is more distinct in the winter because of the strong wind and weak currents in the Gulf of Thailand. Similarly, the wind drift plays a minor role in the summer because of weak wind in the summer and strong currents in the middle of the South China Sea. Therefore, wind drift is more important in conditions of strong winds and weak currents.

This result also means that the ocean currents play a decisive role in dispersing plastic particles in this study. It should be noted that the wind in the South China Sea is particularly important in the generation of ocean currents. This is the reason why in winter the ocean currents go southwest downwind, and also in summer the currents drift to the northeast downwind.

Figure 4.9 shows that the density of the particles decreases exponentially with depth. Specifically, most of the particles are located in the depth of 0 to 5 meters, very few particles reach a depth of 10 meters. This distribution is also similar to a study by *Kooi et al.* (2016) on the distribution of buoyant microplastics with depth in the North Atlantic subtropical gyre. The microplastic particles in that study ranged in size from 0.5 to 5.0 mm, and had the shape of 'fragments' and 'lines'. That study took into account sea states. The result indicated that microplastic concentrations decreases exponentially with depth, with both sea state and particle properties and mostly in the range from 0 to 5m depth.

As mentioned in the introduction, the wind drift factor make up between 1 and 6 % of the wind. This parameter is adjusted depending on each specific object. For example, in oil spill simulations, wind drift factor of 3% is commonly used (*van der Mheen et al.*, 2020). In my study, despite floating on the sea, plastic particles do not rise above the seawater (like empty bottles/ ships) to be directly pushed by the wind. Additionally, due to the small plastic particles they are easily pulled up and down by the disturbance of sea water (*Van Sebille et al.*, 2020). Therefore, I use wind a drift factor of 2%. This is also the default value in OpenDrift model.

5.5 The importance of vertical mixing

The results in figure 4.10 indicate that vertical mixing plays a particularly important role in the drift of marine plastics. The reason for this difference is due to the vertical distribution of the particles. The particles in the scenarios with vertical mixing sink between 0 and 5 meter depth, fig. 4.11. These particles are less likely to be pushed by wind drift, which acts few tens of centimeters below sea surface. Whereas, particles in the scenario without vertical mixing float on the surface. They are all pushed by the wind drift.

In the previous part I have concluded that wind drift is only important in conditions of strong winds and weak currents. However, if we combine the influences of both vertical mixing and wind drift, we can see some conclusions as follows. Without wind drift, the particles only drift with ocean currents. With both vertical mixing and wind drift, the particles drift mainly with ocean currents. This is because the particles sink due to vertical mixing, and the wind drift does not have much effect on the particles below the surface. However, with wind drift and without vertical mixing, the particles would float and wind drift would be significantly important. So both of these factors are important in the drift of marine plastics, and how important these factors are depends on assumptions or how the OpenDrift model set up.

5.6 The importance of biofouling

Biofouling is the growing of organisms on plastic particles which adds mass, causes changes in overall buoyancy of the bio-fouled particle, increasing settling velocity (*Kaiser et al.*, 2017; *Lobelle et al.*, 2021). However, our understanding of the sinking rate of bio-fouled particle is relatively limited. Different approaches result in widely different sinking rates. Despite contradict results, I had used a wide range of terminal velocities to examine the sinking of plastics. If I used high vertical velocity, the particles would sink to the sea floor right at the mouths of the Mekong. Also, if I used too low terminal velocity, the particles would drift in the water like buoyant particles in the previous sections 4.3. The simulations with constant terminal velocities of 1, 2 and 5 m/d are the most informative results. It should be noted that in these simulations, the sinking of particles does not depend on size, shape or density as what I mentioned in the introduction part, but the physical forces (ocean currents, wind drift, vertical mixing, terminal velocity) acting on the particles. Also, the sinking rate is the sum of terminal velocity and vertical velocity.

In all simulations, the blue particles (suspended in water) are mostly concentrated in the deep waters, 1000-4000 meter (figure 4.12). Due to the deep water, these particles need more time to reach the bottom. Meanwhile, the black particles on the sea floor are distributed mainly on the southern continental shelf of the South China Sea where the depth below 150 meter. At this depth, 15 months are long enough for the particles to reach the sea floor. In areas of great variation in depth, such as the Paracel and Spratly Islands and the western coast of the Philippines and Malaysia (figure 2.1), there is a relatively balanced presence of both blacks and blues. This probably due to the relative balance between shallow and deep waters.

In the scenarios of terminal velocities of 1 and 2 m/d, the particles sink slowly, so

they have more chances to drift to many places in the South China Sea. In contrast, in the scenario of 5m/d, due to the strong sinking rate and shallow waters, the particles are deposited almost right after leaving the Mekong, very few particles can travel far. In this 5m/d scenario, the black particles in the east of the Mekong mouths are those released in the summer, and those in the south and the west of the Mekong mouths are released in the fall. This also can be seen in the clips in the footnote in section 4.9.

In these simulations I assume that the particles are already biofouled and the terminal velocities are constant. In fact, the micro-plastic particles need weeks to be biofouled after being released into the marine environment. It is probably more realistic that a few weeks to a few months after the particles are released, the particles begin to sink. Additionally, the sinking rate is also usually not constant, they sink faster at the surface layers and then slow down due to cooler temperatures and less light (*Kaiser et al.*, 2017).

I also assume that if the particles hit the seafloor, they would be permanently stranded there. This is probably not realistic. When plastics reach the seafloor, they can be trapped and transported by further forces. They usually do not deposit in places with gentle slopes. Plastics tends to be deposited in places with steep slopes or in the deep seas (*Barrett et al.*, 2020). This is contrary to my results that the plastic particles tend to deposit in shallow and flat waters (the southern continental shelf of the South China Sea).

Chapter 6

CONCLUSION

The above results bring the following conclusions. Firstly, the seasonal drifts show that during the summer, the plastic particles from the Mekong river drift mainly to the northeast, and in the winter they drift to the southwest. This is because the South China Sea is influenced by the monsoon system, in which the southwesterly wind prevails in summer, and the northeasterly wind dominates in the winter. It should be noted that the drift in winter is less realistic than in the summer, because the plastics mainly drift to the sea in the summer due to the flood season *Haberstroh et al.* (2021).

Secondly, the 15-month simulation shows that more than half of the particles drift out of the South China Sea, and some of them leak to the Pacific and Indian oceans. Also, the Philippines is most vulnerable to marine plastic pollution from the Mekong river.

Thirdly, when considering the stranding of particles, most of the plastics (97%) are stranded after 15 months, and the average travelling time is 3.7 months. Again, the Philippines is most vulnerable to marine plastic pollution from the Mekong river. In this scenario, particles that come ashore will be stranded and stay there indefinitely. In practice, some plastics, after being stranded, can return to the sea under favorable conditions. Also, the stranding and the return of plastics back to the sea depend on both the particles themselves (shape, size, buoyancy, plastic bags, bottles) and characteristics of the coast (substrates, grass, soil, sand, mangrove, rock). However, this is not solved in this study.

Next, rivers play a role in dispersing plastic waste. Specifically, rivers disperse plastics more efficiently. Also, the frequencies of freshwater also affect the dispersal of marine plastics. However, in the long term, 15 months, the influence of rivers or river frequencies on the trajectory of the plastics is insignificant. The influence of river and river water frequency can be seen more clearly in the area around the Mekong and for a short time.

Wind drift and vertical mixing can have combined effects on the trajectory of marine plastics, especially when wind drift is enabled and vertical mixing is disabled. This scenario produces a great difference in the trajectories of the particles. Over time, in the long term, the influence of these factors tends to decrease.

In the biofouling simulations, the results show that the southern continental shelf of the South China Sea is most vulnerable to the plastics pollution due to shallow waters. Meanwhile, in the deep waters, or in the middle of the South China Sea, 15 months of drifting is not long enough for the particles to reach the sea floor. My findings

are contrary to findings by *Barrett et al.* (2020) that plastics tends to be deposited in places with steep slopes or in the deep seas. It should be noted that the results of my simulations are highly dependent on assumptions. Some of the assumptions are the constant terminal velocities of 1, 2 and 5 m/d, the particles are already biofouled as they released on the sea, and the particles would be disable when hitting the sea floor.

Bibliography

Barrett, J., Z. Chase, J. Zhang, M. M. Holl, K. Willis, A. Williams, B. D. Hardesty, and C. Wilcox (2020), Microplastic Pollution in Deep-Sea Sediments From the Great Australian Bight, *Frontiers in Marine Science*, *7*, doi:10.3389/fmars.2020.576170. 1.2, 5.6, 6

Bermúdez, J. R., and P. W. Swarzenski (2021), A microplastic size classification scheme aligned with universal plankton survey methods, *MethodsX*, *8*, 10–15, doi:10.1016/j.mex.2021.101516. 5.1

Brekke, C., M. M. Espeseth, K. F. Dagestad, J. Röhrs, L. R. Hole, and A. Reigber (2021), Integrated Analysis of Multisensor Datasets and Oil Drift Simulations—A Free-Floating Oil Experiment in the Open Ocean, *Journal of Geophysical Research: Oceans*, *126*(1), 1–26, doi:10.1029/2020JC016499. 3.3.1

Cushman-Roisin, B. (2011), *Introduction to geophysical fluid dynamics : physical and numerical aspects*, *International geophysics series*, vol. vol. 101, 2nd ed. ed., Academic Press, Amsterdam. 1.2, 5.3

Dagestad, K. F., J. Röhrs, O. Breivik, and B. Ådlandsvik (2018), OpenDrift v1.0: A generic framework for trajectory modelling, *Geoscientific Model Development*, *11*(4), 1405–1420, doi:10.5194/gmd-11-1405-2018. 3.1.1, 3.1.2

Egbert, G. D., and S. Y. Erofeeva (2002), Efficient Inverse Modeling of Barotropic Ocean Tides, *Journal of Atmospheric and Oceanic Technology*, *19*(2), 183–204, doi:10.1175/1520-0426(2002)019<0183:EIMOBO>2.0.CO;2. 3.1.3

Haberstroh, C. J., M. E. Arias, Z. Yin, T. Sok, and M. C. Wang (2021), Plastic transport in a complex confluence of the Mekong River in Cambodia, *Environ. Res. Lett*, *16*(9), doi:10.1088/1748-9326/ac2198. (document), 1.1, 1.2, 2.5, 3.1.2, 6

Harris, P. T., J. Tamelander, Y. Lyons, M. L. Neo, and T. Maes (2021), Taking a mass-balance approach to assess marine plastics in the South China Sea, *Marine Pollution Bulletin*, *171*(February), 112,708, doi:10.1016/j.marpolbul.2021.112708. (document), 1.1, 1.2

Hole, L. R., K. F. Dagestad, J. Röhrs, C. Wettre, V. H. Kourafalou, Y. Androulidakis, H. Kang, M. L. Hénaff, and O. Garcia-Pineda (2019), The Deepwater horizon oil slick: Simulations of river front effects and oil droplet size distribution, *Journal of Marine Science and Engineering*, *7*(10), 1–20, doi:10.3390/jmse7100329. 3.3.1, 4.5

Jambeck, J. R., R. Geyer, C. Wilcox, T. R. Siegler, A. Andrady, R. Narayan, K. L. Law, and R. Geyer (2015), Plastic waste inputs from land into the ocean Published by : American Association for the Advancement of Science Linked references are available on JSTOR for this article : the ocean Plastic Plastic waste waste inputs inputs from from land into into, *347*(6223), 768–771. (document), 1.1, A1

Kaiser, D., N. Kowalski, and J. J. Waniek (2017), Effects of biofouling on the sinking behavior of microplastics, *Environmental Research Letters*, *12*(12), doi: 10.1088/1748-9326/aa8e8b. 1.2, 4.9, 5.6

Kaiser, D., A. Estelmann, N. Kowalski, M. Glockzin, and J. J. Waniek (2019), Sinking velocity of sub-millimeter microplastic, *Marine Pollution Bulletin*, *139*(December 2018), 214–220, doi:10.1016/j.marpolbul.2018.12.035. 1.2

Khalik, W. M. A. W. M., Y. S. Ibrahim, S. Tuan Anuar, S. Govindasamy, and N. F. Baharuddin (2018), Microplastics analysis in Malaysian marine waters: A field study of Kuala Nerus and Kuantan, *Mar Pollut Bull*, *135*, 451–457, doi: 10.1016/j.marpolbul.2018.07.052. 5.1

Kooi, M., J. Reisser, B. Slat, F. F. Ferrari, M. S. Schmid, S. Cunsolo, R. Brambini, K. Noble, L. A. Sirks, T. E. Linders, R. I. Schoeneich-Argent, and A. A. Koelmans (2016), The effect of particle properties on the depth profile of buoyant plastics in the ocean, *Scientific Reports*, *6*(June), 1–10, doi:10.1038/srep33882. 1.2, 4.8, 5.4

Kooi, M., E. H. Van Nes, M. Scheffer, and A. A. Koelmans (2017), Ups and Downs in the Ocean: Effects of Biofouling on Vertical Transport of Microplastics, *Environ. Sci. Technol*, *51*, doi:10.1021/acs.est.6b04702. 1.2

Kowalski, N., A. M. Reichardt, and J. J. Waniek (2016), Sinking rates of microplastics and potential implications of their alteration by physical, biological, and chemical factors, *Marine Pollution Bulletin*, *109*(1), 310–319, doi:10.1016/j.marpolbul.2016.05.064. 1.2

Kukulka, T., G. Proskurowski, S. Morét-Ferguson, D. W. Meyer, and K. L. Law (2012), The effect of wind mixing on the vertical distribution of buoyant plastic debris, *Geophysical Research Letters*, *39*(7), 1–6, doi:10.1029/2012GL051116. 1.2, 4.8

Kuo, N. J., Q. Zheng, and C. R. Ho (2000), Satellite observation of upwelling along the western coast of the South China Sea, *Remote Sensing of Environment*, *74*(3), 463–470, doi:10.1016/S0034-4257(00)00138-3. 2.2

Lobelle, D., M. Kooi, A. A. Koelmans, C. Laufkötter, C. E. Jongedijk, C. Kehl, and E. van Sebille (2021), Global Modeled Sinking Characteristics of Biofouled Microplastic, *Journal of Geophysical Research: Oceans*, *126*(4), 1–15, doi:10.1029/2020JC017098. 1.2, 4.9, 5.6

Mayer, B., P. E. Damm, T. Pohlmann, and S. Rizal (2010), What is driving the ITF? An illumination of the Indonesian throughflow with a numerical nested model system, *Dynamics of Atmospheres and Oceans*, *50*(2), 301–312, doi:10.1016/J.DYNATMOCE.2010.03.002. 2.3

Md Amin, R., E. S. Sohaimi, S. T. Anuar, and Z. Bachok (2020), Microplastic ingestion by zooplankton in Terengganu coastal waters, southern South China Sea, *Marine Pollution Bulletin*, *150*(April 2019), 110,616, doi:10.1016/j.marpolbul.2019.110616. 1.1

Ng, C. K. Y., P. O. Ang, D. J. Russell, G. H. Balazs, and M. B. Murphy (2016), Marine Macrophytes and Plastics Consumed by Green Turtles (Chelonia mydas) in Hong Kong, South China Sea Region, *Chelonian conservation and biology*, *15*(2), 289–292, doi:10.2744/CCB-1210.1. 1.1

Qi-zhou, H., W. Wen-zhi, Y. S. Li, and C. W. Li (1994), Current Characteristics Of The South China Sea BT - Oceanology of China Seas, pp. 39–47, Springer Netherlands, Dordrecht, doi:10.1007/978-94-011-0862-1_5. (document), 2.3, A8

Qu, X., L. Su, H. Li, M. Liang, and H. Shi (2018), Assessing the relationship between the abundance and properties of microplastics in water and in mussels, *Science of The Total Environment*, *621*, 679–686, doi:https://doi.org/10.1016/j.scitotenv.2017.11.284. 5.1

Röhrs, J., K. F. Dagestad, H. Asbjørnsen, T. Nordam, J. Skancke, C. E. Jones, and C. Brekke (2018), The effect of vertical mixing on the horizontal drift of oil spills, *Ocean Science*, *14*(6), 1581–1601, doi:10.5194/os-14-1581-2018. 1.2, 4.8

Song, Y. K., S. H. Hong, M. Jang, G. M. Han, and W. J. Shim (2015), Occurrence and Distribution of Microplastics in the Sea Surface Microlayer in Jinhae Bay, South Korea, *Arch Environ Contam Toxicol*, *69*(3), 279–287, doi:10.1007/s00244-015-0209-9. 5.1

Sun, J., C. Fang, Z. Chen, and G. Chen (2021), Regional cooperation in marine plastic waste cleanup in the south china sea region, *Sustainability (Switzerland)*, *13*(16), doi:10.3390/su13169221. (document), 1.1, 1.2

Sun, X., Q. Li, M. Zhu, J. Liang, S. Zheng, and Y. Zhao (2017), Ingestion of microplastics by natural zooplankton groups in the northern South China Sea, *Marine Pollution Bulletin*, *115*(1-2), 217–224, doi:10.1016/j.marpolbul.2016.12.004. 1.1

Taufiqurrahman, E., A. J. Wahyudi, and Y. Masumoto (2020), The Indonesian throughflow and its impact on biogeochemistry in the Indonesian Seas, *ASEAN Journal on Science and Technology for Development*, *37*(1), 29–35, doi:10.29037/AJSTD.596. (document), 2.3, A10

Thuy, N., T. Tien, C. Wettre, and L. Hole (2019), Monsoon-Induced Surge during High Tides at the Southeast Coast of Vietnam: A Numerical Modeling Study, *Geosciences (Basel)*, *9*(2), 72, doi:10.3390/geosciences9020072. 2.2, 2.4

Trinh, T. T., C. Pattiaratchi, and T. Bui (2020), The Contribution of Forerunner to Storm Surges along the Vietnam Coast, *Journal of marine science and engineering*, *8*(7), 508, doi:10.3390/jmse8070508. 2.4

van der Mheen, M., C. Pattiaratchi, S. Cosoli, and M. Wandres (2020), Depth-Dependent Correction for Wind-Driven Drift Current in Particle Tracking Applications, *Frontiers in Marine Science*, *7*, doi:10.3389/fmars.2020.00305. 1.2, 3.1.1, 4.7, 5.4

van Sebille, E., S. M. Griffies, R. Abernathey, T. P. Adams, P. Berloff, A. Biastoch, B. Blanke, E. P. Chassignet, Y. Cheng, C. J. Cotter, E. Deleersnijder, K. Döös, H. F. Drake, S. Drijfhout, S. F. Gary, A. W. Heemink, J. Kjellsson, I. M. Koszalka, M. Lange, C. Lique, G. A. MacGilchrist, R. Marsh, C. G. Mayorga Adame, R. McAdam, F. Nencioli, C. B. Paris, M. D. Piggott, J. A. Polton, S. Rühs, S. H. Shah, M. D. Thomas, J. Wang, P. J. Wolfram, L. Zanna, and J. D. Zika (2018), Lagrangian ocean analysis: Fundamentals and practices, doi:10.1016/j.ocemod.2017.11.008. 3.1.1

Van Sebille, E., S. Aliani, K. L. Law, N. Maximenko, J. M. Alsina, A. Bagaev, M. Bergmann, B. Chapron, I. Chubarenko, A. Cózar, P. Delandmeter, M. Egger, B. Fox-Kemper, S. P. Garaba, L. Goddijn-Murphy, B. D. Hardesty, M. J. Hoffman, A. Isobe, C. E. Jongedijk, M. L. Kaandorp, L. Khatmullina, A. A. Koelmans, T. Kukulka, C. Laufkötter, L. Lebreton, D. Lobelle, C. Maes, V. Martinez-Vicente, M. A. Morales Maqueda, M. Poulain-Zarcos, E. Rodríguez, P. G. Ryan, A. L. Shanks, W. J. Shim, G. Suaria, M. Thiel, T. S. Van Den Bremer, and D. Wichmann (2020), The physical oceanography of the transport of floating marine debris, doi:10.1088/1748-9326/ab6d7d. 1.2, 4.9, 5.2, 5.4

Zhang, P., S. S. Wei, J. B. Zhang, Z. Ou, Y. Q. Yang, and M. Y. Wang (2020), Occurrence, composition, and relationships in marine plastic debris on the first long beach adjacent to the land-based source, south China sea, *Journal of Marine Science and Engineering*, *8*(9), 1–15, doi:10.3390/jmse8090666. (document), 1.1

Zhu, C., D. Li, Y. Sun, X. Zheng, X. Peng, K. Zheng, B. Hu, X. Luo, and B. Mai (2019), Plastic debris in marine birds from an island located in the South China Sea, *Marine Pollution Bulletin*, *149*(August), 110,566, doi:10.1016/j.marpolbul.2019.110566. 1.1, 1.2

Appendix

Plastic waste inputs from land into the ocean

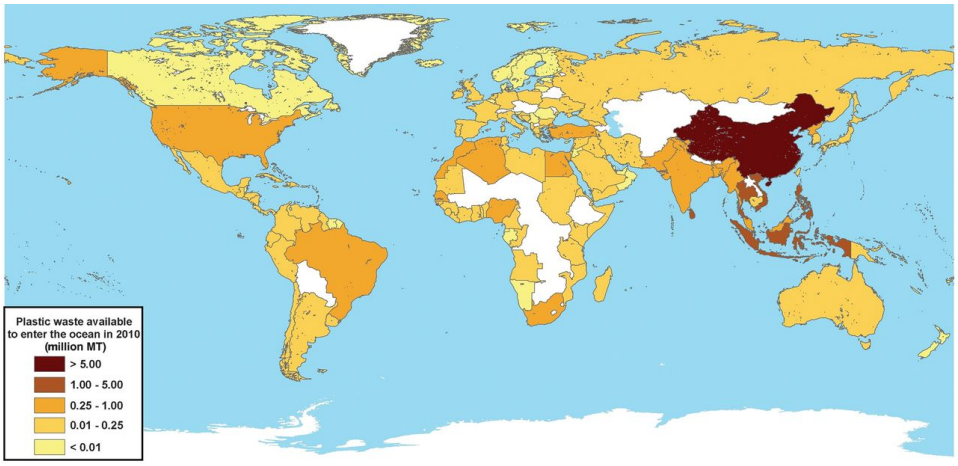

Figure A1: Plastic waste inputs from land into the ocean (Jambeck et al., 2015)

The ROMS domain

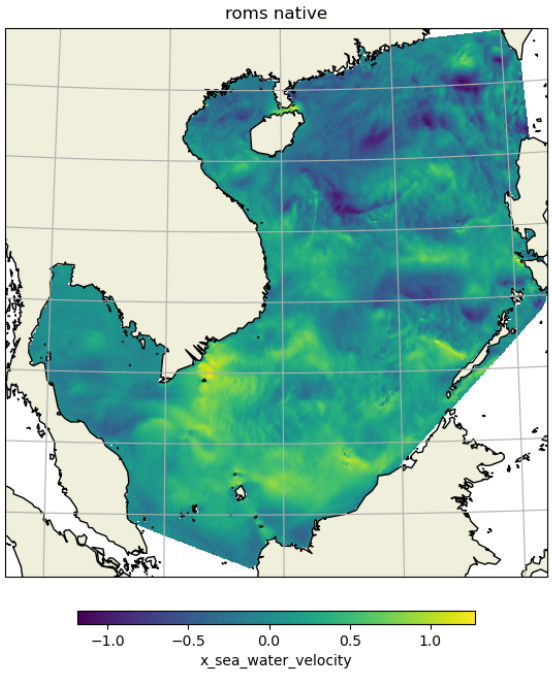

Figure A2: ROMS domain

CMEMS domain

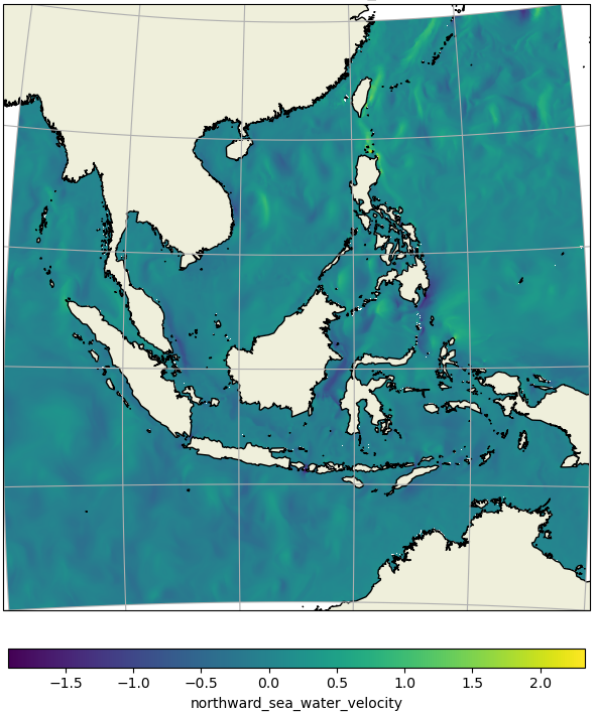

Figure A3: CMEMS dommain

The three biggest rivers in the South China Sea

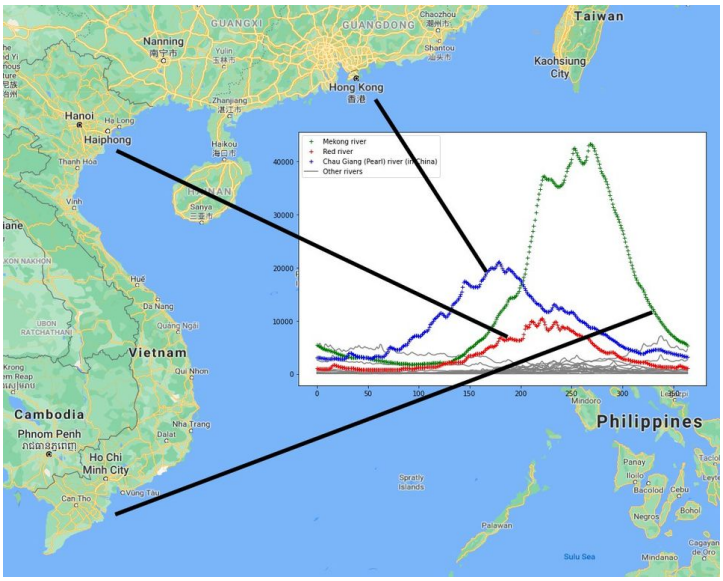

Figure A4: Three biggest rivers in the South China Sea

CMEMS Wind at Vung Tau 2020

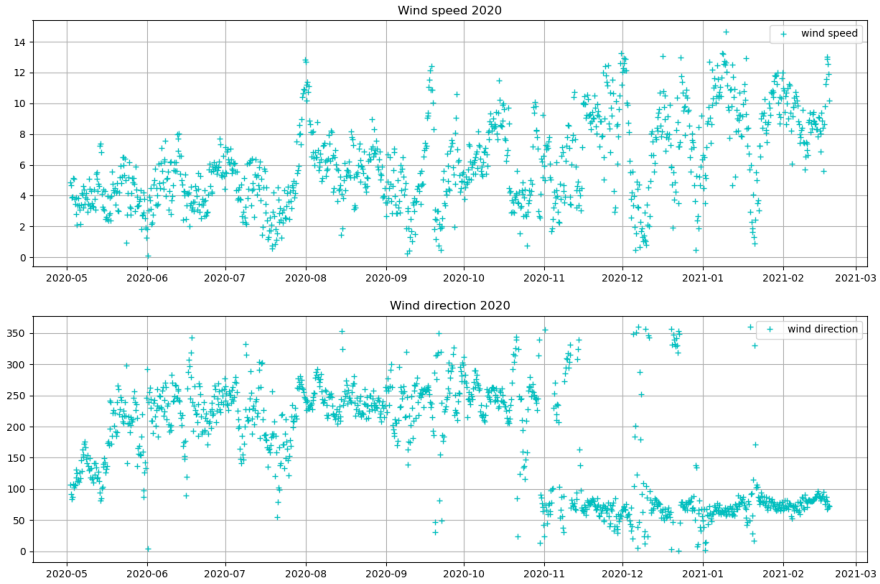

Figure A5: Wind in Vung Tau 2020

CMEMS Waves in Vung Tau in 2021

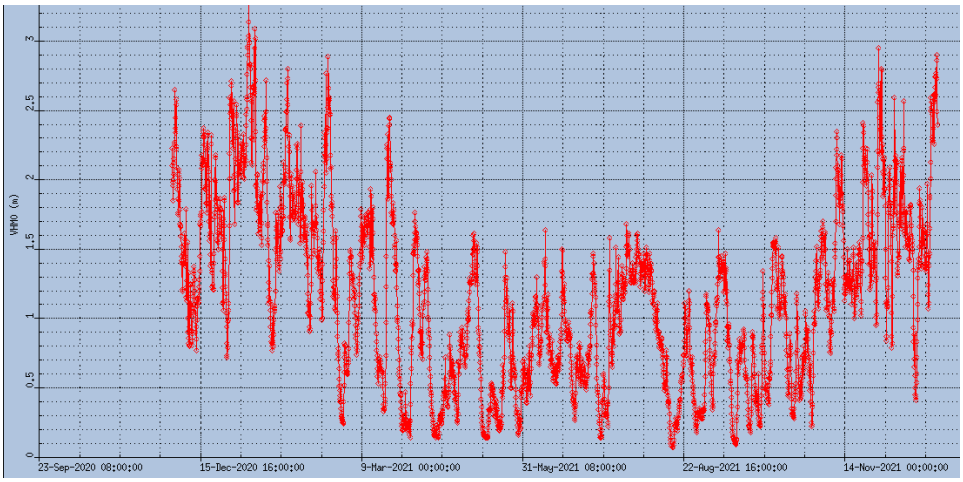

Figure A6: Waves in Vung Tau in 2021

CMEMS sea surface height in Vung Tau

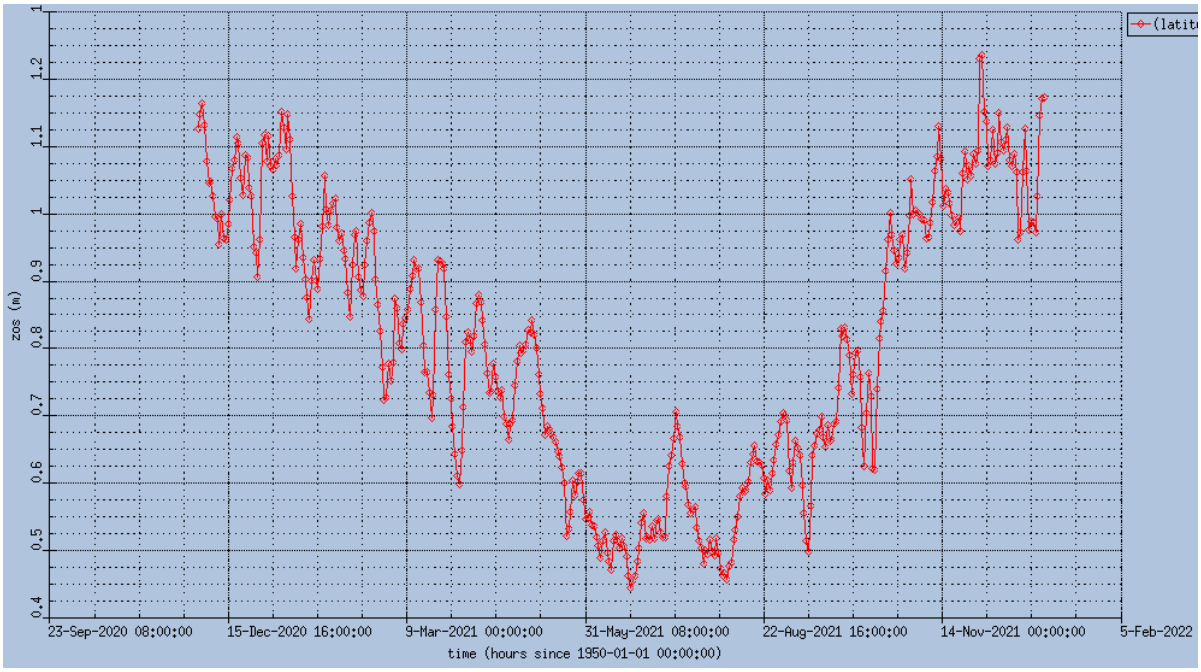

Figure A7: sea surface height in Vung Tau

Circulations in the South China Sea: a) in the winter, and b) in the summer

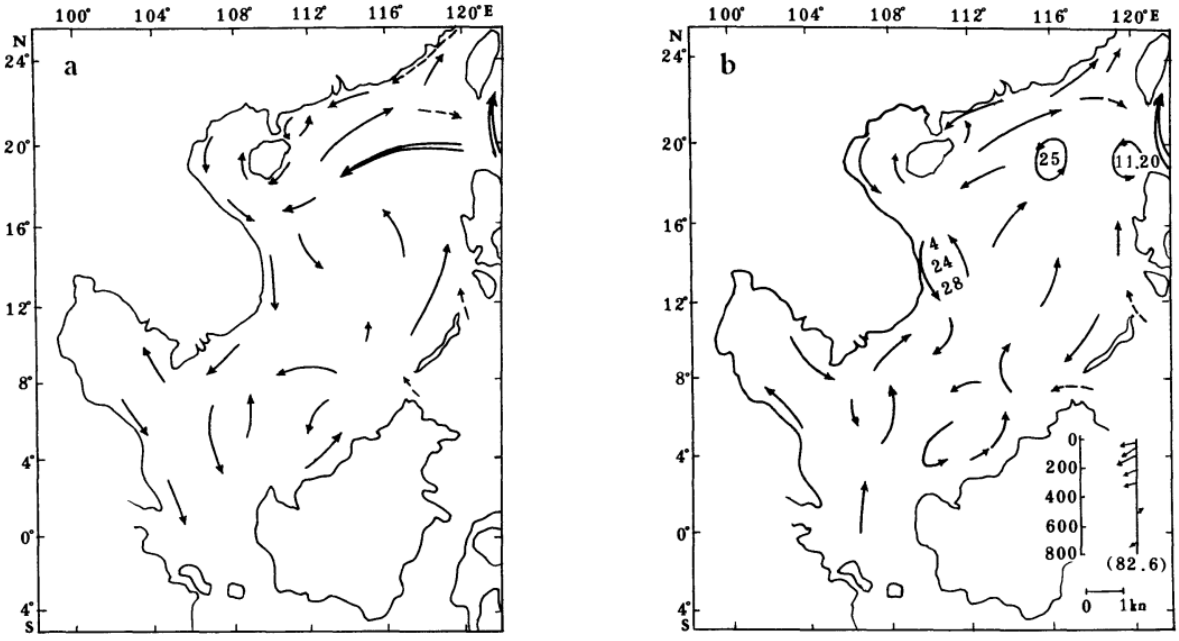

Figure A8: Circulation in the South China Sea (Qi-zhou et al., 1994)

Currents in the summer and winter

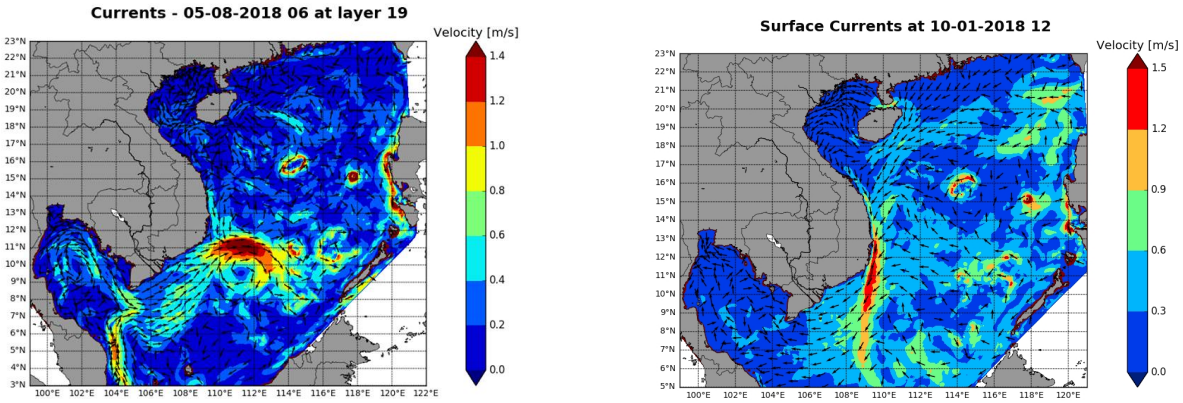

(a) In the summer *(b) In the winter*

Figure A9: Currents in the summer and winter

The Indonesian Throughflow

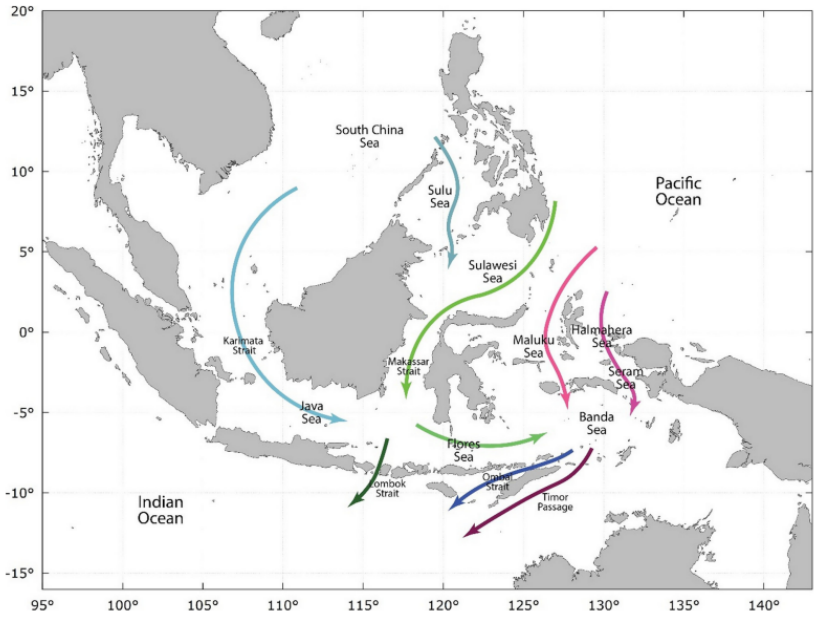

Figure A10: The Indonesian Throughflow (Taufiqurrahman et al., 2020)

13 month observed tides in Vung Tau

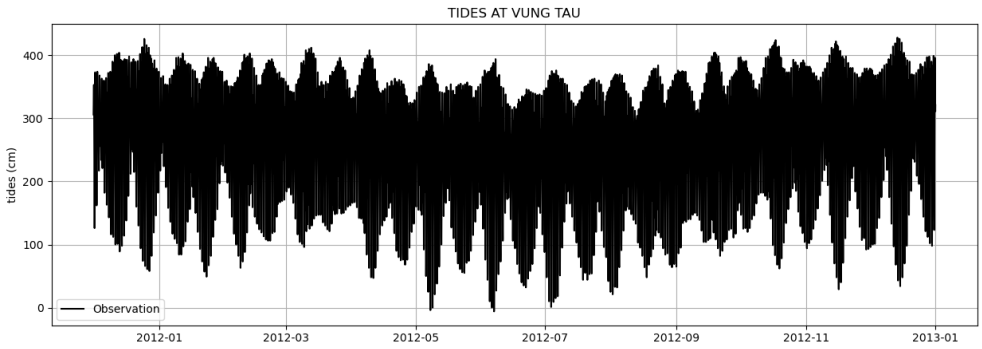

Figure A11: 13 month tides in Vung Tau

The Lower Mekong

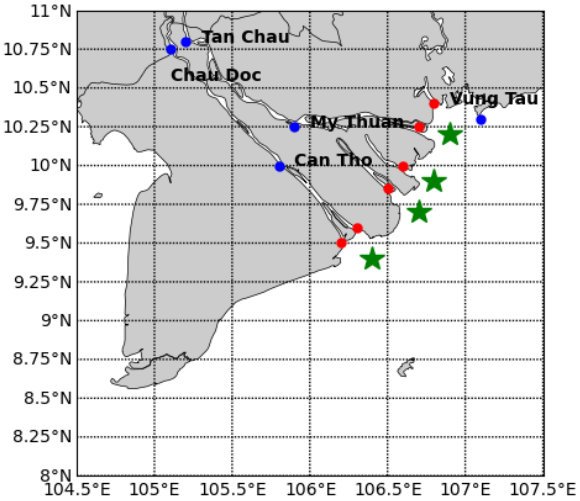

Figure A12: The Lower Mekong and its stations/mouths/sources of plastics

Discharge rates at Mekong mouths

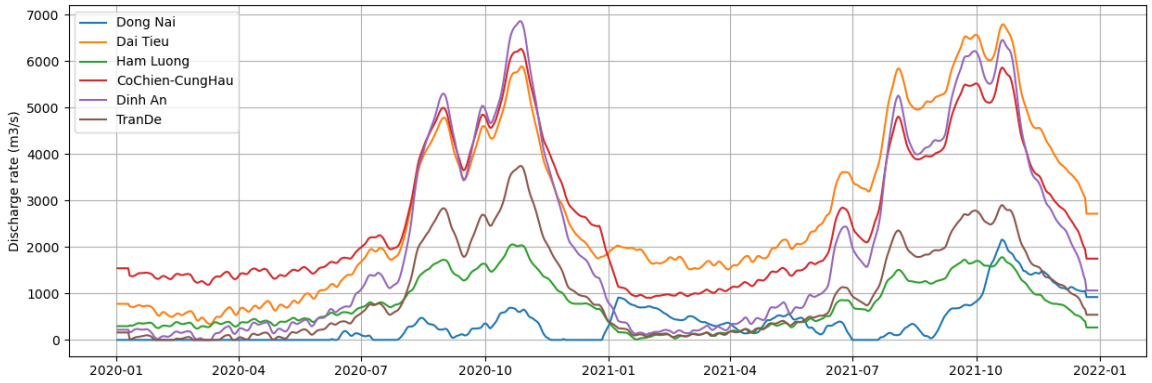

Figure A13: Discharge rates at Mekong estuaries

The ROMS grid

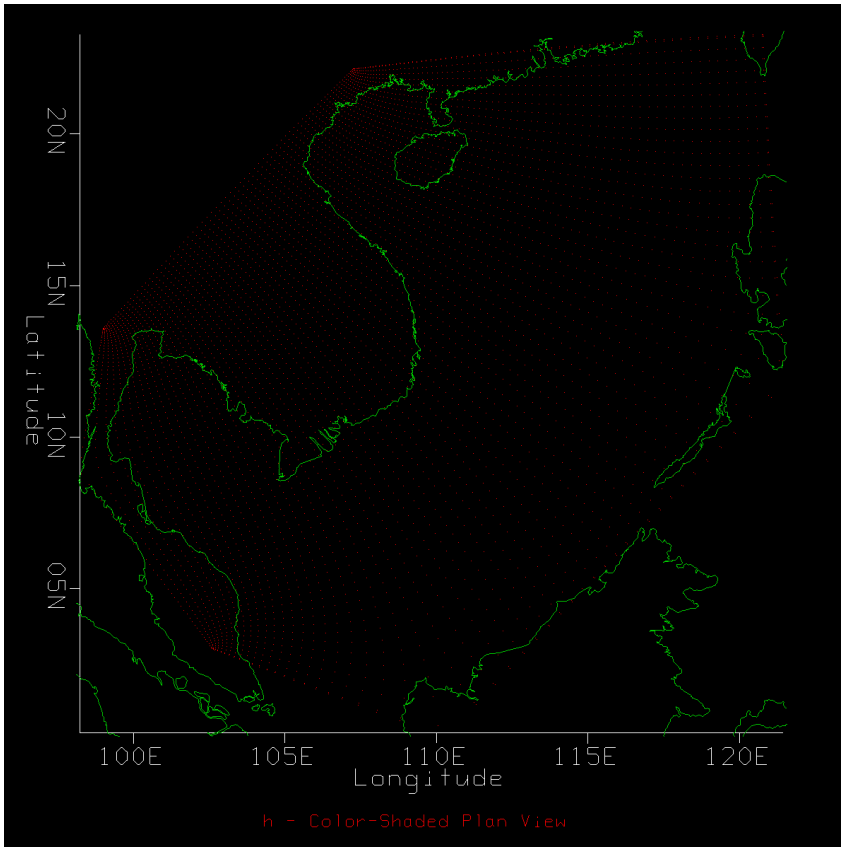

Figure A14: ROMS grid (source: Andrew Walter Seidl, PhD at GFI)

Compare the EFAS with observations at sub-rivers in the Mekong River

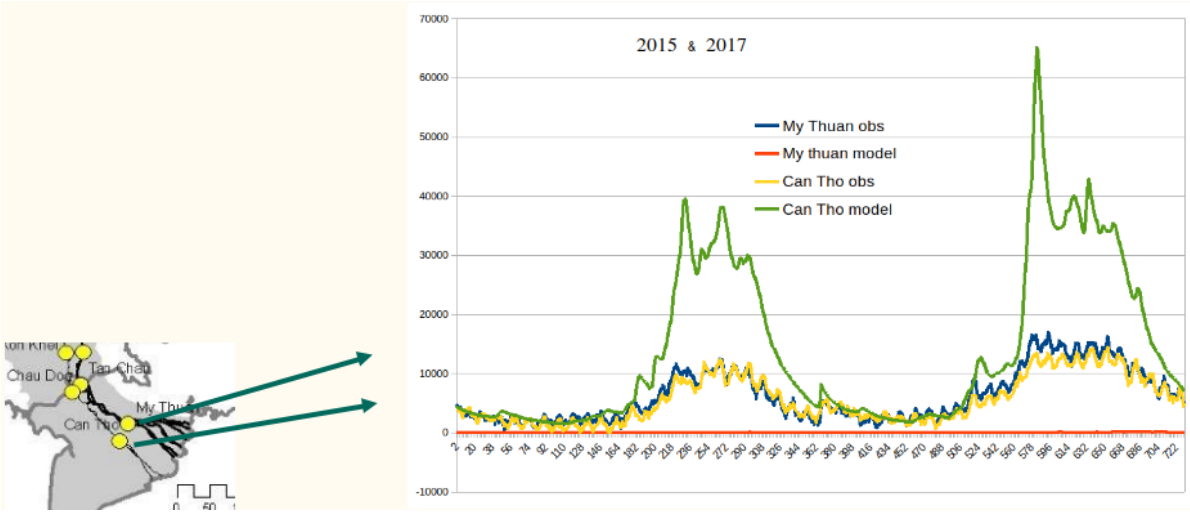

Figure A15: Compare the Global Flood Awareness System with observations in sub-rivers in Mekong River

Compare the EFAS with observations at sub-rivers in the Red River

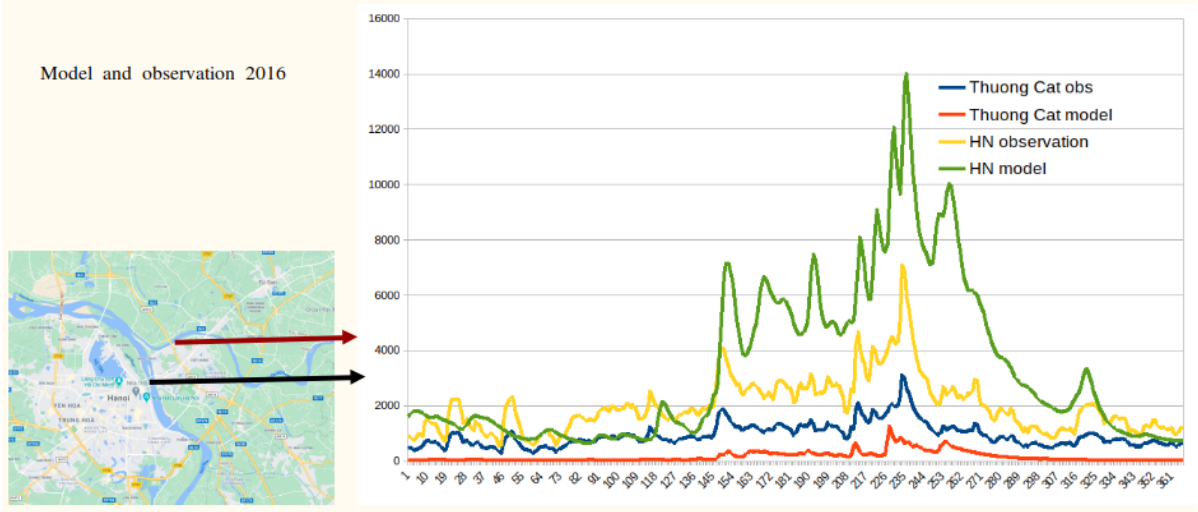

Figure A16: Compare the Global Flood Awareness System with observations in sub-rivers in Red River

The depth of the South China Sea

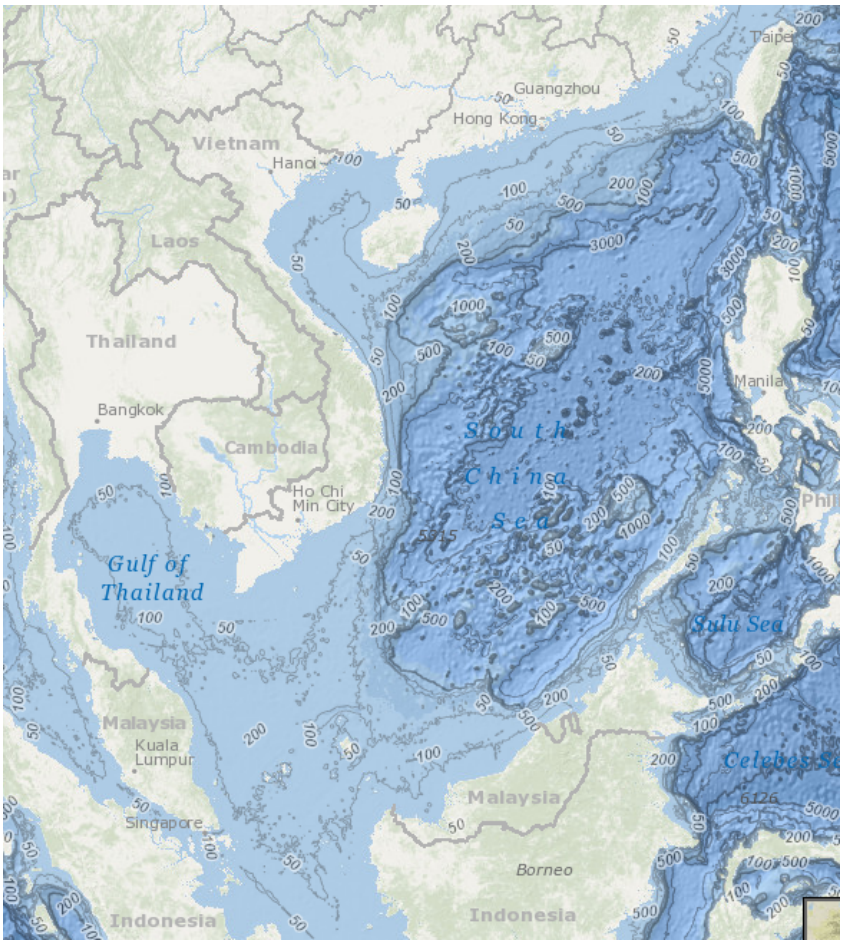

Figure A17: The depth of the South China Sea (source: NOAA)